Chirurgische Klinik und Poliklinik

Klinikum rechts der Isar

Characterization of FoxO3 in ROS and DNA damage-induced hepatocellular carcinoma

Miao Lu

Vollständiger Abdruck der von der Fakultät für Medizin der Technischen Universität München zur Erlangung des akademischen Grades eines Doktors der Medizin genehmigten Dissertation.

Vorsitzende(r): Prof.Dr.Ernst J.Rummeny

Prüfer der Dissertation:

1. Priv.-Doz.Dr.Norbert Hüser
2. Prof.Dr.Helmut Friess

Die Dissertation wurde am 29.07.2016 bei der Technischen Universität München eingereicht und durch die Fakultät für Medizin am 22.02.2017 angenommen.

TABLE OF CONTENTS

ABBREVIATIONS..... 1
1. INTRODUCTION..... 3
1.1 Hepatocellular carcinoma..... 3
1.1.1 Function and architecture of the liver..... 3
1.1.2 Status of hepatocellular carcinoma..... 4
1.1.3 Risk factors of hepatocellular carcinoma..... 4
1.1.4 Pathogenesis of HCC..... 5
1.1.5 LCC and SCC..... 6
1.1.6 Mouse models of HCC..... 7
1.2 Forkhead transcription factor FoxO3..... 10
1.2.1 Forkhead transcription factors..... 10
1.2.2 Forkhead box subclass O..... 10
1.2.3 FoxO signaling pathway in hepatocytes..... 11
1.2.4 FoxO transcription factors and glucose metabolism..... 12
1.2.5 FoxO transcription factors and liver disease..... 13
2. AIMS OF THE STUDY..... 15
3. MATERIALS AND METHODS..... 16
3.1 Materials..... 16
3.1.1 Chemicals and Reagents..... 16
3.1.2 Kit system..... 19
3.1.3 Laboratory equipment..... 19
3.1.4 Consumables..... 20
3.1.5 List of Antibodies..... 21
3.2 Methods..... 23
3.2.1 Animal protocols..... 23
3.2.2 Histology and immunohistochemistry..... 25
3.2.3 RNA-related methods..... 27
3.2.4 DNA related methods..... 31
3.2.5 Protein-related methods..... 32
3.2.6 Statistical analysis..... 34
4 RESULTS..... 36
4.1 FoxO3 expression in human healthy tissue and HCC samples..... 36
4.1.1 Human healthy tissue and HCC samples show no significant difference in mRNA levels of FoxO3..... 36
4.1.2 HCC samples express FoxO3 strongly..... 37
4.2 Hepatic constitutive FoxO3 overexpression leads to liver damage, glucose metabolic dysfunction and morphological alterations..... 38
4.2.1 Hepatic constitutive FoxO3 overexpression mouse model..... 38
4.2.2 Liver-specific FoxO3 overexpression after birth leads to impaired growth..... 40
4.2.3 Liver-specific FoxO3 overexpression after birth leads to liver damage and impaired liver function..... 41
4.2.4 FoxO3 overexpression 5 weeks postoperatively leads to hyperglycemia..... 42

4.2.5 FoxO3 overexpression in hepatocytes leads to morphologic alterations..... 44
4.2.6 FoxO3 overexpression induces elevated expression level of tumor-related genes.....45
4.2.7 FoxO3 is expressed in SCC cells..... 47
4.2.8 Akt is strongly phosphorylated in SCC cells..... 47
4.2.9 Oval cells are not activated in FoxO3CA mice..... 49
4.2.10 Proliferation is impaired in both LCC and SCC areas..... 50
4.2.11 p53-p21 pathway is activated in LCC cells..... 51
4.2.12 FoxO3 activation in SCC areas leads to the expression of markers for DNA damage and HCC..... 53
4.2.13 Hepatic FoxO3 overexpression leads to faster tumorigenesis after DEN injection..... 54
5. DISCUSSION.....57
5.1 Controversial views on the role of FoxO3 in tumorigenesis..... 57
5.2 FoxO3 activation impairs hepatocyte differentiation and liver growth.....58
5.3 Precancerous lesions LCC and SCC induced by FoxO3 over-expression.....59
5.4 Oval cells are not activated in FoxO3CA mice.....60
5.5 ROS and DNA damage are induced by FoxO3CA.....61
5.6 FoxO3 promotes tumorigenesis in DEN-injected mice.....61
5.7 The expression of FoxO3 in human samples.....62
5.8 Conclusion.....63
6. SUMMARY..... 64
7. REFERENCES..... 65
8. CURRICULUM VITAE..... 75
9. LIST OF PUBLICATIONS..... 76
10. ACKNOWLEDGEMENT..... 77

ABBREVIATIONS

8-OHdG	8-hydroxy-2' -deoxyguanosine
γH2AX	phosphorylation of the histone variant H2AX
AFB1	Afatoxin B1
AFP	alpha-fetoprotein
ALT	alanine aminotransferase
AST	aspartate aminotransferase
CK19	Cytokeratin 19
DEN	N-Nitrosodiethylamine
DDR	DNA damage response
DM	diabetes mellitus
DNs	dysplastic foci
DOX	doxycycline
EGF	epidermal growth factor
FGF	fibroblast growth factor
FoxO	Forkhead box subclass O
FoxO3CA	constitutively over expressing activated FoxO3
GADD45	Growth arrest and DNA-damage-inducible protein 45
GAPDH	Glyceraldehyde 3-phosphate dehydrogenase
GEM	genetically engineered HCC mouse models
GPC3	Glypican-3
HBV	hepatitis B virus
HCC	hepatocellular carcinoma

HCV	hepatitis C virus
HE	hematoxylin and eosin
HSCs	hepatic stellate cells
PH3	phosphorylated histone 3
PI3K	Phosphatidylinositol-4,5-bisphosphate 3-kinase
ROS	reactive oxygen species
LAP	liver activator protein
LCC	large cell change
MRI	magnetic resonance imaging
PCNA	proliferating cell nuclear antigen
SA-BETA-GAL	senescence associated beta-galactosidase
SD	standard deviation
SCC	small cell change
SOCS3	Suppressor of cytokine signaling 3
T2DM	type 2 diabetes mellitus
TGFα	transforming growth factor alpha
TLR	toll-like receptor
tTA	tetracycline-responsive transactivator
WT	wild type

1. INTRODUCTION

1.1 Hepatocellular carcinoma

1.1.1 Function and architecture of the liver

The liver is the largest glandular organ in the body and performs multiple critical functions for vital life. First, the liver converts the nutrients absorbed by the small intestine into proper forms that can be used or stored by the body, and removes toxins from the blood. In addition, it produces cholesterol and some important proteins as well as secretes bile, which is helpful for digestion. In addition, the liver is an immunological organ and is selectively enriched in macrophages (Kupffer cells) and lymphocytes (1). Also, the liver is the cornerstone of the coagulation system because it is involved in synthesizing coagulation factors and absorbing vitamin K (2). Finally, the liver is a key organ for metabolic processes.

The liver has complicated histological architectures to execute its various important functions. First, the liver's vascular system is composed of the portal vein, hepatic artery and the hepatic vein. The portal vein conducts blood from the intestines, pancreas and spleen to the liver, which is rich in nutrients absorbed by the intestines and substances secreted by the pancreas and spleen. The hepatic artery supplies the liver with oxygen, and the hepatic vein transports deoxygenated blood and blood that has been filtered by the liver into the inferior vena cava. Second, the liver has a biliary system to transport bile out of the liver. Third, the basic structural and functional unit of the liver is the hepatic lobule (3). A liver lobule is a roughly hexagonal arrangement of hepatocytes arranged outward from a central vein in the center. Between the two cell plates, blood flows from the portal tract to the terminal hepatic venule through the sinusoid vessel.

The liver is composed of many different cell types, which can be divided into

parenchymal cells and non-parenchymal cells. The parenchymal cells are mainly hepatocytes, which constitute about 78% of the liver tissue volume (4); they perform the main functions of the liver, such as protein synthesis, carbohydrate metabolism, lipid metabolism and detoxification. In addition, Non-parenchymal cells accounts for about 6.3% of the liver volume and include endothelial cells, Kupffer cells, hepatic stellate cells, and immunocytes. These cells are involved in controlling immune response in the liver and restoring the liver after damage.

The liver is a special organ with high regenerative capacity. Matured hepatocyte proliferation is the most common way for the liver to restore its mass. However, hepatocyte proliferation could be blocked if the liver injury is too severe or the hepatocytes lose the ability to regenerate. Then, hepatic progenitor cells, also known as oval cells, will be activated and differentiate into hepatocytes and cholangiocytes. Hence, the oval cells express markers for both hepatocytes and cholangiocytes, and oval cell activation is usually accompanied by bile duct reaction.

1.1.2 Status of hepatocellular carcinoma

Hepatocellular carcinoma (HCC) is the fifth-most-common neoplasm and the third-most-common cause of cancer-related death worldwide (5); it was responsible for more than 800,000 deaths in 2013 (6). The incidence of HCC is increasing in many areas, such as parts of Oceania, Western Europe and North America. Incidence rates of HCC almost tripled between 1975 and 2011 (7, 8).

1.1.3 Risk factors of hepatocellular carcinoma

Hepatocellular carcinoma is a heterogeneous cancer with a variety of risk factors. These factors include exposure to hepatitis viruses, vinyl chloride,

tobacco, foodstuffs contaminated with aflatoxin B1 (AFB1), coffee and oral contraceptives; heavy alcohol intake; nonalcoholic fatty liver disease; diabetes; obesity; diet; and hemochromatosis (9).

As mentioned above, the liver is a multifunctional organ involved in energy metabolism, and hepatocytes deal with complicated metabolic procedures. HCC is very likely to be correlated to metabolic disorders. Diabetes mellitus (10) is the most common metabolic disease. Some researchers have tried to determine the relationship between HCC and DM. A meta-analysis shows that diabetes is associated with moderately increased risk of not only HCC prevalence but also HCC mortality (11). Another study revealed that diabetes mellitus is associated with more advanced lesions and poor outcomes in patients with HCC (12). However, the mechanism for how diabetes promotes the initiation of HCC is still not known.

1.1.4 Pathogenesis of HCC

Although HCC tumors can be found in strictly healthy livers, such as fibrolamellar HCC and hepatocellular adenomas (10, 13), HCC is mainly caused by chronic liver disease. Most HCC samples develop from advanced liver fibrosis and cirrhosis, which could be induced by chronic hepatitis B and C and alcohol-related liver disease (14). HCC cells are malignant transformed hepatocytes. The malignant transformation of hepatocytes may occur regardless of the etiological agent through a pathway of increased liver turnover, induced by chronic liver injury and regeneration in a context of inflammation and oxidative stress (15). Chronic liver injury promotes chromosomal aberrations and DNA damage. DNA damage could trigger a series of reaction events called the DNA damage response (DDR) pathways, which include DNA repair, cell cycle arrest and, in the end, cell death or senescence (16-18). However, constant DNA damage may result in genetic alterations and genomic instability, including DNA mismatch repair defects and

impaired chromosomal segregation, the overexpression of growth and angiogenic factors, and tolermerase activation. Genetic alterations such as the overexpression of growth factors and oncogenes and the inactivation of tumor suppressor genes ultimately lead to the malignant transformation of hepatocytes.

1.1.5 LCC and SCC

Huge progressions in HCC treatment have been made during the past years. Tumor resection, liver transplantation and radiofrequency ablation are considered effective managements for early-stage HCC therapy, with five-year survival rates of 60-80% (19, 20). However, the average survival time of advanced HCC is less than 1 year, and the 5-year survival rate is less than 10% (21). It has been reported that only 10% of HCC patients were treated when their cancer was at early stage (22). Hence, it is important to study precancerous HCC lesions, including microscopic dysplastic foci (DF) and microscopic dysplastic nodules (DNs). Based on their cytology and histology, DF usually show large cell change (LCC) and small cell change (SCC).

LCC was first discovered in 1973 and refers to several cellular changes, including nuclear and cytoplasmic enlargement, nuclear pleomorphism and multinucleation (23). Because of the altered phenotype of LCC cells, these were recognized as premalignant changes at first. However, their classifications have evolved as more and more researchers study LCC cells. Lee and colleagues conducted a case-control study, in which they found that LCC cells display a low proliferative rate after KI67 and PCNA staining (24). HBV-related LCC showed higher Tp53 and gamma-H2AX expression, shorter telomere length and decreased senescence-associated beta-galactosidase(SA-BETA-Gal) activity (25). However, no chromosomal abnormalities were found in LCC cells (26). SA-BETA-Gal is a hydrolase that can catalyze the hydrolysis of beta-galactosidase into monosaccharides, but

only in senescent cells. Hence, SA-BETA-Gal is a widely accepted senescence marker. Taken together, it is widely agreed that LCC is not involved in hepatocarcinogenesis. However, people have different opinions on whether LCC is a precursor. Some think LCC would be a common feature of cirrhosis and HCC, but it is not a malignant precursor (24). Rather, it could just result from a disturbance in hepatocellular replication (27). Others still trust that LCC is a direct precursor of HCC (28, 29), because LCC is frequently observed in HCC, especially HBV-related HCC.

SCC was first described in HBV-related chronic hepatitis and cirrhosis in 1983 (30); it is defined as a set of cytological changes, including small cell size, nuclear pleomorphism and increased nuclear/cytoplasmic ratio. It has long been regarded as a precursor of HCC. First, the liver parenchyma of SCC shows cytological and histological similarities with early, well-differentiated HCC (31, 32). Second, SCC was found more frequently in livers than HCC (33). Third, more DNA damage and chromosomal abnormalities were detected in SCC cells (25, 26). In conclusion, SCC could be a precancerous lesion, as opposed to LCC.

1.1.6 Mouse models of HCC

Due to the complexity of hepatocellular carcinoma, the mechanisms underlying HCC are still not well understood. Animal HCC models are an important method to investigate the mechanisms underlying the initiation and progression of HCC because they provide us with an in vivo way to study carcinogenesis. Many animal models of HCC with different species have been developed to better understand the mechanisms of HCC development in recent years. Among them, the laboratory mouse is the most widely used and has many advantages, such as small size and genomic similarities to humans (34). Generally, there are three different types of mouse HCC models, including genetically engineered, xenograft, and carcinogen-induced models.

1.1.6.1 Genetically engineered HCC mouse model

Genetically engineered HCC mouse models (GEMs) have been widely used and well developed in the past few decades, ever since the transgenic technique was discovered in 1980s (35), because GEMs have many advantages compared to other HCC models. GEMs provide a way to study the molecular features of HCC in vivo and can be used to investigate the role of specific genes in combination with a liver-specific carcinogen. Genetic alterations of the genes involved in cellular signaling pathways, such as growth, proliferation, apoptosis and angiogenesis, could lead to the development of HCC. Even until now, the exact signaling pathways that lead to the formation of hepatocellular carcinoma are still not clear, but p53, Rb and Wnt/β-catenin pathways are involved (36-38). Hence, genetic alterations of these pathways will induce HCC and could be regarded as HCC mouse models.

For example, inactive tumor suppressors such as p53, Rb and Pten in mouse liver will induce HCC (39-41). On the other hand, the overexpression of oncogenes such as c-Myc and β-catenin/Ras will also develop into HCC (42, 43). Additionally, researchers have also found that constitutive overexpression of growth factors such as FGF, EGF and TGFα would induce the development of HCC (44-46).

HBV and HCV infections are the risk factors for HCC, and mouse models expressing HBV X protein (HBx) or HCV core protein are also used as mouse HCC models (47, 48). However, HCC induced by HBV and HCV has a special mechanism, compared to other genetically modified mouse models. HBx can activate several genes, such as ICAM-1 and c-myc, to promote cell adhesion and proliferation. The expression of HCV core protein leads to lipid accumulation in hepatocytes by activating PPAR alpha, which could result in HCC genesis.

1.1.6.2 Xenograft mouse models

Xenograft HCC mouse models are the most widely used to induce HCC in mice. It can be easily accomplished by implanting HCC cells or tumor tissue fragments into the recipient mice. Previously, the recipient mice had to be the same strain as the cells or tumor fragments to avoid being eliminated by the activated immune system. However, human HCC cells lines and tissues can now be implanted into immunodeficient mice, including nude mice and severe combined immunodeficient mice. The nude mice are athymic and hairless, and have a deficiency of T lymphocytes, along with impaired T and B cell function (49). The severe combined immunodeficient mice have deficient numbers and function of both T and B lymphocytes (50). These mice allow for xenograft HCC mouse models to be set up with human cancer cells and tissues, and provide a better way for preclinical evaluations of anticancer agents.

1.1.6.3 Carcinogen-induced HCC mouse model

Many chemicals and drugs such as aflatoxins, vinyl chloride and combined oral contraceptives have been proven as carcinogens for human HCC (51). Hence, it is possible to create HCC mouse models with carcinogens. Generally, carcinogens for HCC can be divided into two groups: genotoxic and non-genotoxic carcinogens. Genotoxic carcinogens can form DNA adducts and cause genetic alterations in the hepatocytes, which will eventually lead to the formation of HCC. Non-genotoxic carcinogens promote carcinogenesis by controlling cell proliferation, apoptosis and differentiation (52, 53).

The genotoxic chemical diethylnitrosamine (DEN) has been the most widely used carcinogen to induce HCC in mice since the 1960s (54). DEN-induced tumors are genetically similar to human HCCs with poor survival (55). DEN is able to induce DNA damage and produce reactive oxygen species in hepatocytes, which lead to HCC formation in 80-100% of male mice (56). DEN

can also induce genetic mutations, such as H-ras activating mutation, which is rare in human HCC. DEN works in a dose-dependent manner to induce tumors (57). For example, 84% C57BL6/J mice will get HCC at 40-70 weeks after DEN injection, at a dose of 5 mg/kg (58).

1.2 Forkhead transcription factor FoxO3

1.2.1 Forkhead transcription factors

The forkhead proteins are characterized by a conserved 100-amino acid domain called the forkhead box (59). They are transcription factors that play important roles in many processes, such as developing various organs, regulating cell proliferation, senescence and metabolic homeostasis (60). Fifty forkhead proteins have been identified in the human genome and have been categorized into 19 subclasses (FOXA to FOXS) on the basis of their sequence homology inside and outside the forkhead domain (59-61). Among these 19 subclasses, subclass O has received the most attention in the past decades.

1.2.2 Forkhead box subclass O

The O subclass of the forkhead transcription family (FoxO) acts as a central key point in an array of cellular functions, such as glucose metabolism, cell cycle and apoptosis. There are four members in the FoxO subgroup: FoxO1 (FKHR), FoxO3A (FKHRL1), FoxO4(AFX) and FoxO6. FoxO1, FoxO3 and FoxO4 are expressed in most organs and tissues at different levels (62). In contrast, FoxO6 is mainly expressed in some parts of the brain (63). FoxO4 is abundant in skeletal and cardiac muscle, and FoxO3 is abundant in cardiac and neuronal tissues. FoxO factors perform overlapping functions, and it is still unknown whether they share same target genes or not.

1.2.3 FoxO signaling pathway in hepatocytes

FoxO transcription factors serve as a counterpoint to Akt in controlling cell proliferation and gluconeogenesis, which can be regulated by insulin and the other growth factors through the PI3K/AKT signaling pathway (Figure 1).

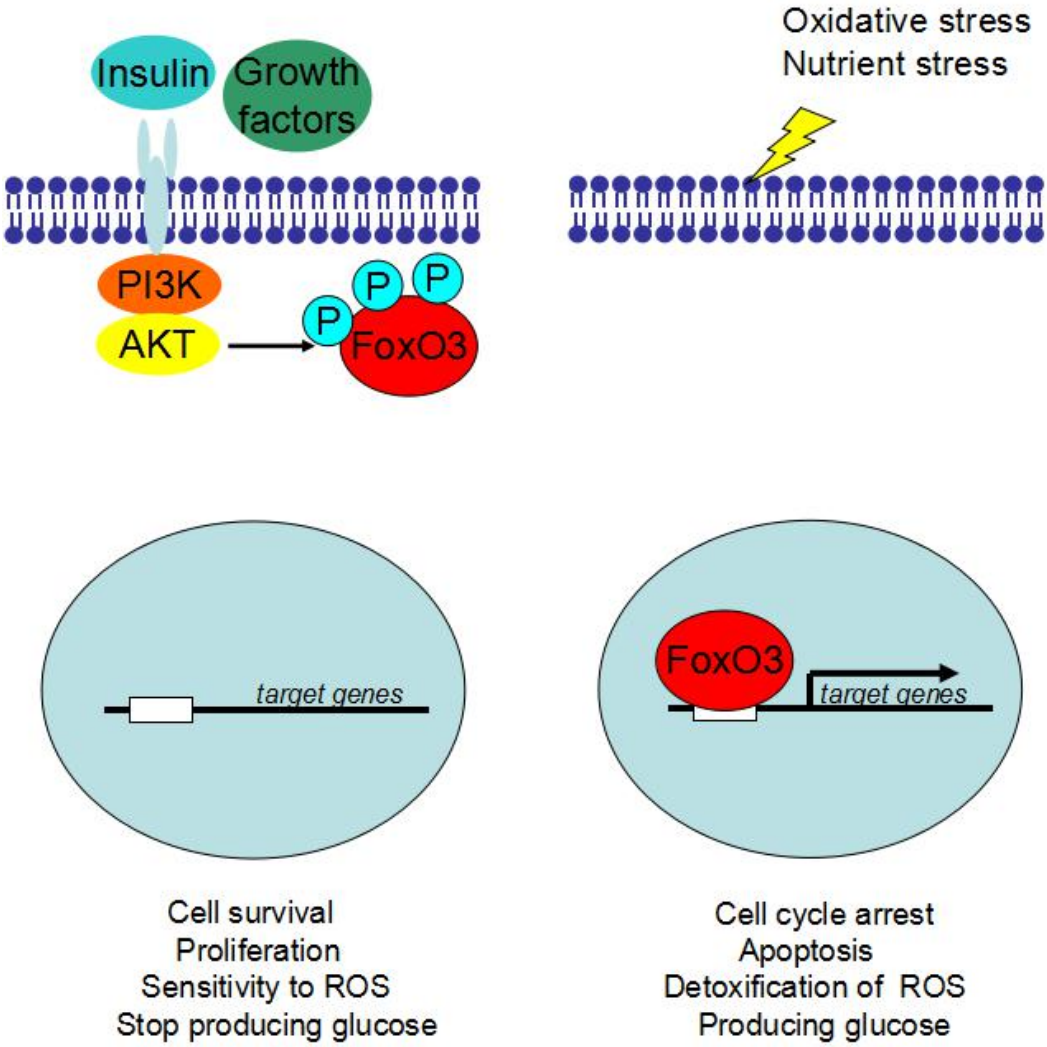

Figure 1. FoxO signaling pathway in hepatocytes.
FoxO3 activity in hepatocytes is regulated by the PI3K/Akt signaling pathway. When PI3K/Akt is activated by insulin or other growth factors, FoxO3 is phosphorylated and inhibited in the cytoplasm. When hepatocytes are under oxidative or nutrient stress, FoxO3 is activated in the nucleus.

Growth factors such as insulin can activate phosphoinositide kinase (PI3K) and the downstream serine/threonine kinase Akt. Activated Akt can inhibit FoxO proteins by phosphorylating them by specific sites. For FoxO3, Akt can phosphorylate FoxO3 protein at three conserved amino acids, including Threonine32, Serine253 and Serine315. When FoxO factors are phosphorylated, they are transported from the nucleus to the cytoplasm by interacting with 14-3-3 proteins, which function as molecular chaperons (64). FoxO inhibited in the cytoplasm would lead to cell survival, proliferation, sensitivity to reactive oxygen species (ROS) and the stopped production of glucose. On the other hand, when hepatocytes suffer from starvation and ROS stress, FoxO proteins will be activated in the nucleus, and the downstream targets of FoxO transcription factors will be expressed. FoxO proteins activated in the nucleus would induce cell cycle arrest, apoptosis, the detoxification of ROS and glucose production by hepatocytes.

1.2.4 FoxO transcription factors and glucose metabolism

FoxO transcription factors play an important role in glucose homeostasis, and FoxO1 has gained the most attention. Activated FoxO1 binds to the FoxO-responsive elements in the promoter region of glucose-6-phosphatase (G6P) and cytosolic phosphoenolpyruvate carboxykinase (PCK1), which lead to increased hepatic glucose production (65, 66). Liver-specific knockout of FoxO1 leads to hypoglycemia, decreased gluconeogenic gene expression and enhanced glucose tolerance (67). Interestingly, hepatic FoxO1 deletion in diabetic mice rescues the diabetic phenotype of insulin resistance by decreasing the gluconeogenic gene expression (68). In addition, FoxO1 is a pivotal factor for regulating beta-cell compensation to insulin resistance in the pancreas (69, 70). As mentioned above, the different members of the FoxO subclass have overlapping functions, and the other FoxO members also play roles in glucose metabolism. Hepatic FoxO6 knockout mice showed poor

gluconeogenesis and reduced ability to produce glucose in response to glucagon (71). It has been also reported that liver-specific knockout FoxO1/3/4 mice had lower blood glucose levels under both fasting and unfasting conditions, and they failed to develop type 2 diabetes after being fed with a high-fat diet (72). FoxO3 activation led to hyperglycemia, hyperinsulinemia, impaired glucose tolerance and insulin sensitivity in hepatocytes of mouse liver with a tet-off system that overexpress a constitutive, activated form of FoxO3 (73).

1.2.5 FoxO transcription factors and liver disease

In addition to metabolic issues, FoxO proteins were also found to be involved in several liver diseases, such as hepatitis C infection, fibrosis and HCC.

FoxO1 can be activated directly by hepatitis C virus (HCV), which could lead to insulin resistance. HCV core protein could suppress Akt activity due to the upregulation of FoxO1 expression (74). Also, FoxO1 nuclear accumulation and activation can also be achieved through increased HCV NS5A-mediated ROS production and JNK activation (75). FoxO3 also plays a role in HCV infection. It regulates the innate immune signaling pathway by suppressing TLR signaling (76). FoxO3 was activated by starvation/malnutrition in HCV infection and this could increase the expression of SOCS3 and suppress the interferon signaling pathway (77).

FoxO transcription factors also play a potential role in fibrosis because FoxO proteins are essential for the quiescent stage of long-living cells such as hematopoietic stem cells (78). Hepatic stellate cells (HSCs) were found to be regulated by FoxO1. Hyperinsulinemia could inactivate FoxO1 in HSCs, which would lead to the activation of HSCs and may result in fibrosis in nonalcoholic fatty liver disease (79).

FoxO proteins were also found to be involved in tumor genesis and development. FoxO3a has gained the most attention within the FoxO family.

Apoptosis-related genes such as PUMA and Bim are downstream targets of FoxO3 (80). Inhibiting FoxO3a could promote cell proliferation and tumorigenesis (81). However, since the FoxO family is involved in many cellular functions, the role that FoxO3 plays still remains unclear. Also, there is still no evidence to show how FoxO3 protein is expressed in HCC patients.

2. AIMS OF THE STUDY

The FoxO signaling pathway is known to play an important role in many regulatory processes, including hepatocyte regulation. FoxO3 works as a tumor suppresser in different cancers, such as cholangiocarcinoma, non-small cell lung cancer and prostate cancer (82-85). However, the role of FoxO3 in HCC development and progression is still not fully understood.
I hypothesize that FoxO3 may be an important cornerstone in hepatocarcinogenesis and may be even used as a marker of HCC development.

Consequently, the aims of the present study can be formulated as follows:

1. What is the expression of FoxO3 in human HCC, and is there any detectable difference between HCC and normal tissue samples?

2. Does FoxO3 overexpression lead to increased liver damage and metabolic dysregulation in a mouse model of constitutive FoxO3 overexpression?

3. Is there a time-dependent impact of FoxO3 overexpression on morphological alteration and functional dysregulation in this mouse model?

4. Does FoxO3 overexpression lead to an increased expression of tumor-related genes, and is there any relation to the development of the precursor lesions of HCC development?

3. MATERIALS AND METHODS

3.1 Materials

3.1.1 Chemicals and Reagents

Table 1. Chemicals and reagents

Chemicals and Reagents	Supplier
0.25% trypsin/EDTA	Invitrogen (Carlsbad,CA,USA)
2-Mercaptoethanol	Sigma-Aldrich (St.Louis,Mo, USA)
6x DNA Loading Dye	Thermo Scientific
Acetic acid	Merck Biosciences (Darmstadt, Germany)
Acetic anhydride	Sigma-Aldrich
Acrylamide solution	ROTH (Karlsruhe,Germany)
Agarose	ROTH
Ampicillin	Sigma-Aldrich
Ammonium persulfate (APS)	Sigma-Aldrich
Bovine serum albumin (BSA)	ROTH
Bromophenol blue	Sigma-Aldrich
Calcium chloride	Merck Biosciences
Citric acid	ROTH
DAB+ Chromogen	DAKO
Dream Taq™ Green PCR Master Mix	Fermentas
ECL detection reagent	Amersham

Eosin	Sigma-Aldrich
Ethanol	Roth
Formamide	Merck Biosciences
Gelatine	Roth
GeneRiler™ DNA Ladder	Thermo Scientific
Glycine	Roth
Haematoxylin	Merck Biosciences
Hydrochloric Acid	Hauseigene Apotheke
Hydrogen peroxide (30%)	Roth
Histowax	Leica (Wetzlar, Germany)
Humidified chamber	TeleChem (Sunnyvale, CA, USA)
Isoflurane	CP-Pharma (Burgdorf, Switzerland)
Isopropanol	Roth
Laurylsulfate (SDS)	Sigma-Aldrich
Liquid Nitrogen	Tec-Lab (Taunusstein,Germany)
Liquid DAB & Chromogen Substrate	DakoCytomation
Methanol	Merck Biosciences
Milk Powder Blotting Grade	Roth
MOPS	Roth
Mounting Medium	DAKO
N-Nitrosodiethylamine	Sigma-Aldrich
Nitrocellulose Membranes	Bio-Rad
Normal Goat Serum	DAKO
NuPAGE LDS Sample Buffer	Invitrogen

NuPAGE Sample Reducing Agent	Invitrogen
PageRuler™ PlusPrestained Protein Ladder	Thermo
Para-formaldehyde	Apotheke TU München
Phosphate Buffered Saline (PBS) pH7.4	Invitrogen
Potassium Chloride (KCL)	Merck Biosciences
Protease Inhibitor Cocktail Tablet	Roth
Proteinase K	Sigma-Aldrich
RIPA Buffer	Cell Signaling
RNAse DNAse-free Water	Invitrogen
Roticlear	Roth
SDS Ultra Pure	Roth
Sodium Chloride	Merck Biosciences
Sodium Citrate	Merck Biosciences
Sodium Hydroxide	Merck Biosciences
Sodium Phosphate	Merck Biosciences
Sucrose	Sigma-Aldrich
TEMED	Merck Biosciences
Tris Base	Merck Biosciences
Triton 100x	Roth
Tween 20	Roth

3.1.2 Kit system

Table 2. Kits

Kit	Supplier
BCA Protein Assay Kit	Thermo Scientific
Qiagen DNA Mini Kit	Qiagen
QIAquick Purification Kit	Qiagen
QuantiTect Reverse Transcription Kit	Qiagen
RNeasy Plus Mini Kit	Qiagen
SYBR Green Master Kit	Roche Diagnostics
BCA Protein Assay Kit	Thermo Scientific
QIAGEN DNA Mini Kit	Qiagen

3.1.3 Laboratory equipment

Table 3. Laboratory equipment

Name	Supplier
Analytic balance	METTLER (Giessen, Germany)
Balance	SCALTEC (Goettingen,Germany)
Biophototer	Eppendorf (Hamburg, Germany)
Centrifuge	Eppendorf
CO_2 incubator	SANYO (Secausus, NJ, USA)
Electrophresis / Electroblotting equipment / power supply	Invitrogen
Freezer -20 °C	LIEBHERR (Bulle，Switzerland)
Freezer -80 °C	Heraeus (Hanau, Germany)

Glucosemeter	Abbott
Lightcycler 480	Rochediagnostics(Penzberg, Germany)
Microplate Reader	Thermo Scientific
Microscope	Leica (Wetzlar, Germany)
Microwave oven	SIEMENS (Munich, Germany)
Nanodrop	Thermo Scientific
PH-meter	Thermo Scientific
Refrigerator 4 °C	COMFORT (Buller, Switzerland)
Roller mixer	STUART (Stone, UK)
Scanner	Canon (Tokyo, Japan)
Sterilgard Hood	Thermo Scientific
Thermomixer	Eppendorf
Vortex Mixer	NEOLAB (Heidelberg, Germany)
Water Bath	LAUDA (Koenigshofen, Germany)
Tissue embedding machine	Leica
Tissue processor	Leica
Vacuum tissue processor ASP200s	Leica

3.1.4 Consumables

Table 4. Consumables

Name	Supplier
Cell scraper	SARSTEDT (Nuembrecht, Germany)
Coverslips	MENZEL (Braunschweig, Germany)
Filter (0.2μm)	NEOLAB (Heidelberg, Germany)

Hyperfilm	GE Healthcare
Pure Nitrocellulose membrane	BIO-RAD
Sterile needles	BD (Franklin Lakes, NJ, USA)
Tissue culture dishes	GREINER (Frickenhausen,Germany)
Tissue culture flasks	GREINER
Tissue culture plates (6-well)	GREINER
Falcon tubes (15ml, 50ml)	GREINER
Blotting paper	Whatman (Maidstone, Kent, UK)

3.1.5 List of Antibodies

3.1.5.1 Primary antibodies

Table 5. First antibodies

Name	Catalog number	Application	Supplier
8-Hydroxyguanosine	ab-48508	IHC (1:3000)	Abcam
AFP	AF5369	IHC (1:200)	R&D
Cytokeratin 19	Ab-53119	IHC (1:200)	Abcam
FoxO3a (H144)	sc-11351	IHC (1:200)	Santa Cruz
FoxO3a(D19A7) Rabbit mAb	#12829	IHC(1:2000) WB (1:1000)	Cell Signaling
Ki67 (SP6)	RM-9106	IHC (1:200)	Thermo Scientific
p21 (F-5)	sc-6246	IHC (1:200)	Santa Cruz
p53 (CM5)	NCL-p53-CM5p	IHC (1:800)	Leica
Phospho-Akt(Ser	#4060	IHC (1:200)	Cell Signaling

473)			
Phospho-Histone H3	#9701	IHC (1:1000)	Cell Signaling

3.1.5.2 Secondary antibodies

Table 6. Secondary antibodies

Name	Catalog number	Application	Supplier
Goat HRP- Labelled Anti-Mouse Ab#	K4001	IHC (1:5000)	Dako Deutschland GmbH (Hamburg, Germany)
Goat HRP- Labelled Anti-Rabbit Ab#	K4003	IHC (1:5000)	Dako Deutschland GmbH
Sheep HRP-Labelled Anti-Mouse Ab#	NA931	WB (1:5000)	GE Healthcare (Little Chalfont, UK)
Sheep HRP-Labelled Anti-Rabbit Ab#	NA934	WB (1:5000)	GE Healthcare

WB = western blot; IHC = Immunohistochemistry; Ab# = antibody

3.1.5.3 Primer sequence for real time PCR

Table 7. Primer sequence

Gene(specie)	Sense (5' →3')	Antisense (5' →3')
AFP(M)	ATGAAACCTATGCCCCTCCC	TCAGGCTTTTGCTTCACCAGG
c-Myc(M)	ATGCCCCTCAACGTGAACTTC	CGCAACATAGGATGGAGAGCA
CD13(M)	AATCTCATCCAGGGAGTGACC	GTGGCTGAGTTATCCGCTTT
CD133(M)	TCATCGCTGTGGTCGTCATTG	GTCCGCTGGTGTAGTGTTGTAG
CD24a(M)	TCACCACAAGCACCAAATTC	ATTAGCCAAGGCCAACATGA
CD49(M)	ATTCAGGAGTAGCTTGGTGGAT	AGCGCTTAAAGAATCCACACTT

CD90(M)	GGTGGCAGAAGAAGACAAGG	CCTTCCTGCACGGACTTAGA
FoxO3(H)	CTTCAAGGATAAGGGCGACA	CGACTATGCAGTGACAGGTTG
GAPDH(H)	GGAGCGAGATCCCTCCAAAAT	GGCTGTTGTCATACTTCTCATGG
GAPDH(M)	AGGTCGGTGTGAACGGATTTG	TGTAGACCATGTAGTTGAGGTCA
GPC3(M)	CAGCCCGGACTCAAATGGG	CAGCCGTGCTGTTAGTTGGTA
H19(M)	GAACAGAAGCATTCTAGGCTGG	TTCTAAGTGAATTACGGTGGGTG
P53(M)	CTCTCCCCCGCAAAAGAAAAA	CGGAACATCTCGAAGCGTTTA
Perp(M)	ATCGCCTTCGACATCATCGC	CCCCATGCGTACTCCATGAG
Pten(M)	TGGATTCGACTTAGACTTGACCT	GCGGTGTCATAATGTCTCTCAG
Kras(M)	CAAGAGCGCCTTGACGATACA	CCAAGAGACAGGTTTCTCCATC
Sca1(M)	GTTTGGGATGGCCTGATGT	GGTTGGGGTTCAGAGTTAAGG

M=Mus musculus; H=Homo sapiens

3.2 Methods

3.2.1 Animal protocols

3.2.1.1 FoxO3 constitutively over-expressing mouse model

In our study, we set up a FoxO3 constitutive overexpression mouse model by crossbreeding tetracycline-responsive transactivator (75) mice with mice bearing a constitutively active human FoxO3 allele (FoxO3CA) under the control of a tTA-regulated promoter (86, 87). tTA expression is controlled by the rat liver activator protein (LAP) to achieve a hepatocyte-specific FoxO3 overexpressing model (73, 88). My mice are of C57BL/6 background and kept in an animal facility at the Technische Universität München. Experiments were carried out under a protocol approved by the Animal Studies Committee (Regierung von Oberbayern, no. 55.2-1-54-2532-164-2014) and in accordance with the institutional guidelines.

3.2.1.2 Doxycycline administration

Our mouse model used a tTA-induced tet-off system to achieve controlled FoxO3 gene expression. Doxycycline (DOX) was administered in the mice models' drinking water at a concentration of 0.1 mg/ml, supplemented with 10 mg/ml sucrose in dark bottles during embryogenesis and lactation. FoxO3 could be overexpressed by abolishing DOX feeding. In our study, FoxO3CA was closed during the embryonic and postnatal periods until the different experiment time points we required. In this study, we activated FoxO3 overexpression at two different time points: immediately after birth and at 5 weeks old.

3.2.1.3 DEN injection

N-Nitrosodiethylamine (DEN) was used to induce HCC tumors in this study. The mice were injected with 10 mg/kg DEN intraperitoneally when they were 15 days old. When they were around 4 weeks old, we analyzed the genotype. According to their genotype, the mice were divided into two groups: the FoxO3CA group and the wild-type (WT) group. DOX water was supplied until they were 5 weeks old. Then, they were fed with normal water, and FoxO3CA was activated in hepatocytes.

3.2.1.4 Tissue collection

Before sacrificing the mice, they were fasted for 6 hours but supplied with normal water. Then, their blood glucose levels were measured with a glucose meter from the tail vein. Afterwards, the mice were anaesthetized with isofluran and sacrificed through cervical dislocation. Blood was taken from the angular vein of the mice. Then, the livers were harvested, and one lobe of each liver was kept in paraformaldehyde (PFA) stored at 4 °C, and the rest of the lobes

were frozen with liquid nitrogen and kept at -80 °C. Serum was collected by centrifuging blood at a speed of 7,000 rpm for 6.5 minutes.

3.2.1.5 Biochemical analysis

Transaminases including alanine-aminotransferase (ALT), aspartate-aminotransferase (AST) and cholesterol were measured by the Rechts der Isar hospital clinical laboratory.

3.2.1.6 Magnetic resonance imaging

Magnetic resonance imaging (MRI) scanning was performed to check the HCC induced by DEN injection in the mice by the Institute of Radiology, Kilinikum rechts der Isar.

3.2.2 Histology and immunohistochemistry

3.2.2.1 Paraffin sections

After the fixation with 4% PFA overnight, the tissues were trimmed and fixed into appropriate sizes and shapes, and placed in embedding cassettes. Then, the samples went through ascending alcohol rows to dehydrate, using an automatic tissue processor and the following steps.

70% ethanol, once for 1 hour

96% ethanol, 2 changes, once for 1 hour, once for 45 min

100% ethanol, 2 changes, once for 1 hour, once for 45 min

Xylene, 2 changes, 1 hour each

Paraffin wax (60 ºC), twice for 15 min, once for 30 min and once for 1 hour.

Then, the tissue samples were embedded into paraffin blocks. After cooling

down to -15 °C, the blocks were cut into 2.5 µm sections. The sections were moved to an incubator for drying at 37 °C.

3.2.2.2 Hematoxylin and eosin staining (HE staining)

Paraffin-embedded tissue sections were deparaffinized with Roticlear three times for ten minutes each. Afterwards, the tissues were rehydrated using a descending alcohol row. Then, the slides were stained in hematoxylin solution for 30 seconds and washed in running tap water for at least 15 minutes. The slides were counterstained in eosin for 5 seconds. They were washed in tap water shortly and then dehydrated in ascending alcohols, with a final immersion in Roticlear three times. Finally, the slides were mounted with Vectashield mounting medium.

3.2.2.3 Immunohistochemistry (IHC) staining

Immunohistochemistry staining was performed with the Dako Envision System (DakoCytomation GmbH, Hamburg, Germany).

- Constitutive paraffin-embedded tissue sections (2.5 µm thick) were deparaffinized with Roticlear three times for ten minutes each and rehydrated with a descending alcohol row (two minutes each).
- Antigen retrieval was performed by retreating the slides in citrate buffer (pH 6.0; 10 mM citric acid) in a 600 °C microwave oven for 15 minutes. Then, the slides were put on a bench for at least 30 minutes to cool down.
- The slides were washed in TBS for 5 minutes and blocked with 3% peroxidase, which was diluted with absolute methanol for 10 minutes in the dark. Slides were then washed again in TBS 3 times, for 5 minutes each time.
- The reaction was blocked with TBS/3% BSA or TBS/10% goat serum for 1 hour at room temperature.

- The primary antibodies were diluted to recommended concentrations in blocking solution, pipetted onto the slides and incubated overnight at 4 °C in a wet box.
- The slides were rinsed three times with TBS/0.1 BSA and incubated with horseradish peroxidase HRP-conjugated secondary antibody for 1 hour at room temperature.
- The slides were washed with TBS/0.1 BSA three times. Then, an enzymatic reaction with substrate solution (0.5 mg DAB/phosphate buffer) was performed in the slides. The reaction was stopped in water when it was ready.
- The tissue was dehydrated in ascending alcohol rows (two minutes each) and cleared in Roticlear three times, for ten minutes each.
- Finally, the slides were mounted with Vectashield mounting medium.

3.2.3 RNA-related methods

3.2.3.1 RNA isolation

Total RNA was extracted from collected mouse and human liver tissue with an RNeasy Mini Kit (Qiagen) according to the manufacturer's instructions.

- Around 30 mg of mouse or human liver tissue was placed in 400 µL RLT with 0.4 µL β-ME. The lysate was homogenized and then centrifuged for 3 min at maximum speed. The supernatant was carefully collected, and the rest was discarded.
- One volume of 70% ethanol was added to the lysate and mixed by pipetting. Up to 700 µl of the sample was transferred to an RNeasy Mini spin column placed in a 2 ml collection tube and centrifuged for 15 seconds at 8500 x g. The flow-through was discarded.
- Then, 700 µl Buffer RW1 was added to the column. The lid was closed, and the sample was centrifuged for 15 s at 8500 x g. The flow-through was

discarded.

- Next, 500 µl Buffer RPE was added to the RNeasy spin column. The lid was closed, and the contents were centrifuged for 15 s at 8500 x g. The flow-through was discarded.
- Afterwards, 500 µl Buffer RPE was added to the RNeasy spin column. The lid was closed, and the contents were centrifuged for 2 min at 8500 x g. Then, the RNeasy spin column was placed in a new 2 ml collection tube and centrifuged at full speed for 1 min to dry the membrane.
- The RNeasy spin column was placed in a new 1.5 ml collection tube. Next, 30 µl RNase-free water was added to the spin column membrane. The lid was closed, and the contents were centrifuged for 1 min at 8500 x g to elute the RNA.

The RNA samples were stored in the fridge at −80 °C.

3.2.3.2 Evaluation of RNA quality and cDNA synthesis

The RNA concentrations were tested using the NanoDrop (Thermo Scientific, Wilmington, USA). The absorbance proportion at 260 nm and 280 nm wavelengths were used to evaluate the RNA's quality. A ratio of around 2.0 was recommended as pure RNA.

The RNA was reverse transcribed with the QuantiTect Reverse Transcription Kit. The steps are as follows.

- Eliminate genomic DNA in RNA.

Component	Volume	Final concentration
Template RNA	Variable (1µg)	
RNase-free water	Variable	
gDNA wipeout buffer	2 µl	1x
Total volume	14 µl	

- The reaction mix was incubated for 2 minutes at 42 °C, and afterwards put on ice immediately.
- The reverse transcription mix was made.
-

Component	Volume	Final concentration
DNA elimination reaction mix	14 µl	
Quantiscript reverse transcriptase	1µl	
Quantiscript RT buffer	4 µl	1x
RT primer mix	1 µl	
Total volume	20 µl	

- The reaction mix was incubated for 15 minutes at 42 °C in and then incubated for 3 minutes at 95 °C using inactive Quantiscript reverse transcriptase. The final cDNA concentration was adjusted to be lower than 50 ng/µl and stored at −20 °C.

3.2.3.3 Quantitative real-time PCR

Quantitative real-time PCR (qRT-PCR) was carried out using a LightCyclerTM480 system with the SYBR Green 1 Master Kit (Roche Diagnostics, Penzberg, Germany). The cycle threshold (CT) value described the cycle of the PCR in which the fluorescence signal became significant.

qPCR reaction mix

SYBR Green SuperMix	12.5 µl
Primers	2 µl
cDNA template	5 µl
ddH_2O	3 µl
Total	25 µl

qPCR reaction program

Procedure	Temperature	Duration
1. Activation	55 °C	2 minutes
2. Denaturation	94 °C	10 minutes
3. Denaturation	94 °C	15 seconds
4. Annealing	55 °C	30 seconds
5. Elongation	72 °C	30 seconds
	40 cycles for 3 – 5 steps	
6. Elongation	72 °C	10 minutes
7. Conservation	4 °C	

3.2.4 DNA related methods

3.2.4.1 DNA isolation

A piece of 0.5 cm mice tail was cut for DNA isolation. First, tails were digested in 500 µl STE buffer and 20 µl proteinase K in a 55 °C incubator overnight. After incubation, the samples were centrifuged at full speed for 10 min, and the supernatant was transferred into new tubes with 400 µl of isopropanol to precipitate the DNA. After ten minutes of incubation at room temperature, the samples were centrifuged at full speed at room temperature again, the supernatant was discarded and the remaining DNA pellets were washed with 70% ethanol twice. The tubes were dried in a 37 °C incubator; afterwards, 50 µl Dnase-free water was added to resuspend the DNA. The DNA samples were stored at 4 °C until use.

STE buffer

NaCl	0.1 M
Tris-Hcl	10 mM
EDTA	1 mM
SDS	1 %
pH	8
Aqua dest	Various

3.2.4.2 Genotyping

The transgenes tTA and FOXO3CA were detected by PCR with specific pairs of primers according the following protocols.

Reaction mix

PCR Master Mix, 2x	12.5 µl
Sense primer (10 µM)	0.5 µl
Antisense primer (10 µM)	0.5 µl
DNA template	1 µl
RNase-free water	10.5 µl
Total volume	25 µl

Primer sequences:

tTA 5´ gctaggtgtagagcagcctacattg

tTA 3´ gtccagatcgaaatcgtctagcgcg

FOXO3-P17 catggagtctgcggccgtctcc

FOXO3-P48 ggtacccggggatcctctagtcag

PCR programs

Procedure	Temperature	Duration
1. Starting	94 °C	3 minutes
2. Denaturation	94 °C	45 seconds
3. Annealing	62 °C	45 seconds
4. Elongation	72 °C	80 seconds
	40 cycles for 2-4 steps	
5. Elongation	72 °C	2 minutes
6. Conservation	4 °C	

3.2.5 Protein-related methods

3.2.5.1 Protein extraction from liver tissue

All of the liver tissue lysates were made from snap-frozen tissue with RIPA

buffer (cell signaling). A piece of frozen liver tissue weighing 50 mg was put into 350 µl RIPA buffer with a steel ball. Then, the tissue was disrupted with a homogenizer for 3 minutes. Afterwards, the sample was put on ice for 40 minutes and then centrifuged at full speed for 20 minutes at 4 °C. The supernatant was taken carefully and kept at −80 °C until use.

3.2.5.2 Protein concentration measurement

The BCA Protein Quantification Kit was used to measure the concentration of the protein samples. BCA reagent was freshly prepared by adding 4% $CuSO_4$ to the standard solution and protein solution at a ratio of 1:50. Then, 10 µl of the probe or the standard solution was added to a microtiter 96-well plate and mixed with 200 µl of the prepared BCA solution. After being incubated at 37 °C for 25 min, the extinction was measured at a wavelength of 570 nm and the protein concentration was calculated.

3.2.5.3 SDS-polyacrylamide gel electrophoresis (SDS-PAGE)

First, I prepared the protein denature mix as follows.

Protein denature mix

Protein	Variable (up to 20µg)
Water	16.25 µl-volume of protein
NuPAGE LDS Sample Buffer 4x	6.25 µl
NuPAGE Reducing Agent 10x	2.25 µl
Total volume	25 µl

Second, the mixture was denatured at 70 °C for 10 min. The protein samples were separated according to their size by using a discontinuous gel system, which involved stacking (5%) and separating gel (7.5-10%) layers that differed

in their salt and acrylamide concentrations. 20 µg protein from each sample was loaded into suitable polyacrylamide gel and separated by gel electrophoresis (BioRad, Germany) in running buffer (25 mM Tris, 192 mM glycine, 0.1% SDS, pH 8.3) at 80 V until the samples were focused in the stacking gel, and then the gel was run at 100 V until the target band was at the right position.

3.2.5.4 Immunoblotting

When the target band arrived at the appropriate position, proteins were transferred electrophoretically onto a polyvinylidene fluoride (PVDF) microporous membrane using a Trans-Blot SD Wet Transfer Cell (Bio-Rad). The transfer conditions were 250 mA for 1-2 hours at room temperature, depending on the molecular weight of the target protein. Then, the membrane was blocked with 5% non-fat milk or BSA for 1 hour. Afterwards, the first antibody that was diluted with blocking solution was added to the membrane and kept at 4 °C overnight.

On the second day, the membrane was washed with 0.05% TBST three times for 10 minutes each. Then, secondary antibody diluted with 5% nonfat milk was added to the membrane for 1 hour at room temperature. Afterwards, the membrane was washed again. Signal detection was performed using SuperSignal West Pico Chemiluminescent Substrate according to Thermo-Scientific's instructions. The blots were exposed to an autoradiography film.

3.2.6 Statistical analysis

For statistical analyses, either the GraphPad Prism 5 Software (GraphPad, San Diego, CA, USA) or IBM SPSS 19 Software (Statistical Package for the Social Sciences, IBM, NY, USA) was used. All of the experiments were

conducted in triplicate. An unpaired Student's t-test was performed for group-wise comparisons of two groups. The level of statistical significance was set at $p < 0.05$. The results are expressed as mean ± standard deviation (SD) unless indicated otherwise.

4 RESULTS

4.1 FoxO3 expression in human healthy tissue and HCC samples

4.1.1 Human healthy tissue and HCC samples show no significant difference in mRNA levels of FoxO3

Since FoxO3 is expressed in many cancer types, such as colorectal cancer and breast cancer (89, 90), we checked the expression level of FoxO3 in healthy liver tissue and HCC samples (Department of Surgery, Klinikum rechts der Isar, der Technischen Universität München, Munich; approved by the Ethics Committee, no. 1926/07).

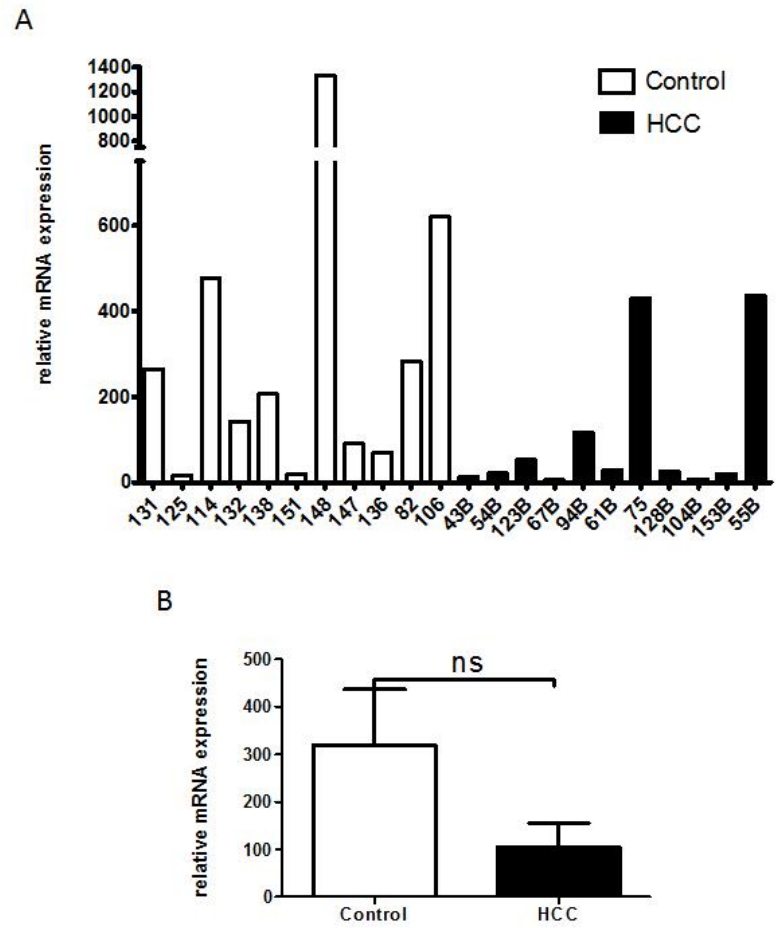

Figure 2: FoxO3 expression in human healthy tissue and HCC samples.

A. Relative mRNA expression levels of FoxO3 in 11 healthy liver samples and 11 human HCC samples, as determined by RT-qPCR. The results were normalized to housekeeping gene GAPDH.

B. Relative mRNA expression level of FoxO3 in control group (healthy liver) and HCC group (n = 11). p = 0.1040; ns = not significant.

We isolated RNA from 11 healthy liver tissues (which were resected within the resection of the liver to achieve safety margin), and 11 HCC samples. Real-time PCR was performed to assess the mRNA level of FoxO3 in these samples (Figure 2A). The expression levels of FoxO3 for the healthy and the HCC groups were hugely different. The FoxO3 mRNA level in HCC group seemed lower than that in healthy group, but the difference was not significant (Figure 2B).

4.1.2 HCC samples express FoxO3 strongly

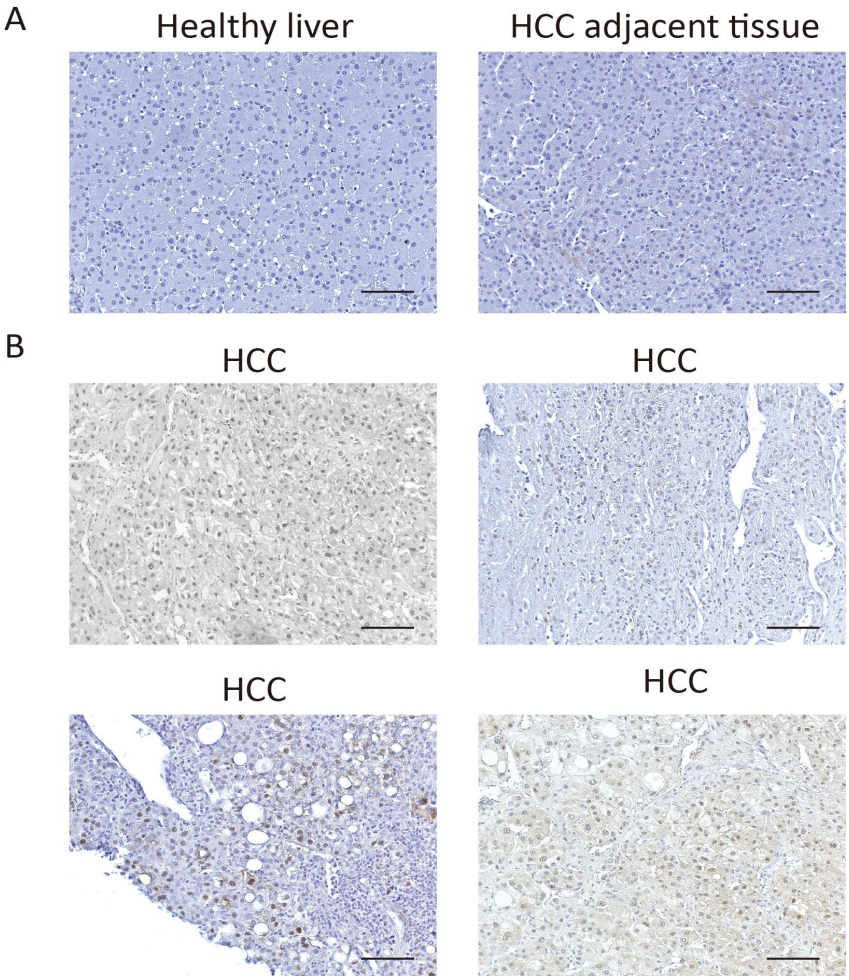

Figure 3. IHC staining of FoxO3 on human sections.

A. IHC staining of FoxO3 was performed on 3 healthy liver tissues and 3 HCC adjacent tissues. FoxO3 was not stained on these sections.

B. The FoxO3 expression of a cohort of 31 HCC patient samples was determined by IHC staining. FoxO3 was expressed in the nuclei of the hepatocytes (scale bar: 100 μm).

The protein expression levels of FoxO3 in human samples were also estimated by immunohistochemistry staining, including healthy liver from non-HCC patients, HCC adjacent samples and HCC samples. Interestingly, we performed FoxO3 IHC staining on 3 healthy liver and 3 HCC adjacent sections, and found that FoxO3 were not expressed in either healthy liver or HCC adjacent liver tissues (Figure 3A). By contrast, when determining FoxO3 expression in 31 HCC samples, FoxO3 was stained in the nuclei of 15 samples (48.4%) (Figure 3B). Because FoxO3 is a transfection factor, it is active in the nucleus and inactive in cytoplasm.

4.2 Hepatic constitutive FoxO3 overexpression leads to liver damage, glucose metabolic dysfunction and morphological alterations.

4.2.1 Hepatic constitutive FoxO3 overexpression mouse model

Since FoxO3 was observed to be activated in human HCC tissues, we set up a hepatic constitutive FoxO3 overexpression (FoxO3CA) mouse model to determine the role that FoxO3 plays in HCC development.

FoxO proteins can be phosphorylated and inhibited by activated Akt (91). Akt can phosphorylate FoxO3 at three specific sites—T32, S253 and S315—and then FoxO3 will be inhibited and translocated into the cytoplasm. To achieve a constitutive active form of FoxO3, we used an active allele of FoxO3, in which those three sites were mutated into alanine (Figure 4A). As a result, once FoxO3 was expressed in our mouse model, it would always be in the active form.

Then, we used the tet-off system to set up a. inducible FoxO3 overexpression mouse model. We crossbred mice expressing tetracycline-regulated transactivator (75) under LAP promoter, which is specifically expressed in the hepatocytes of mice containing the mutated FoxO3 allele and a luciferase reporter gene controlled by a bidirectional promoter, $(tetO)_7$. The tet-off system

can be regulated through administration or deprivation of DOX, which can block the tTA binding (Figure 4B). Our mouse model was confirmed by western blot. Proteins from the wild-type (WT) mice and our FoxO3CA mice were isolated, and the protein level of FoxO3 in the FoxO3CA mice was much higher than that of the WT mice (Figure 4C).

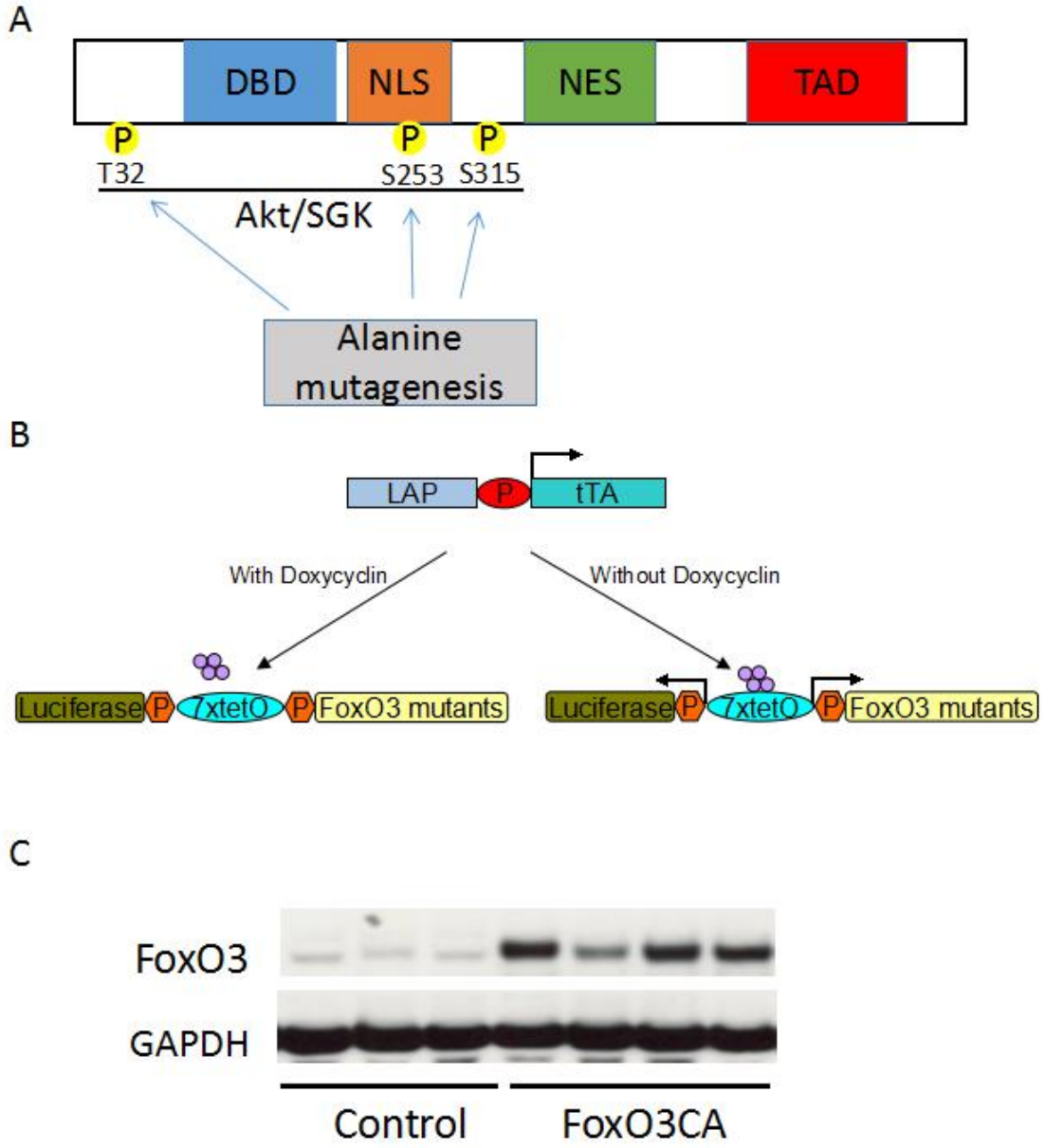

Figure 4. Hepatic constitutively FoxO3 overexpression mouse model

A. Akt phosphorylate sites T32, S253 and S315 in FoxO3 are mutated into alanine residues.

B. Tetracyclin-regulated (tet-off) expression system.

C. Western analysis of whole liver extracts from wild-type mice and FoxO3CA mice using antibodies against FoxO3 and GAPDH. GAPDH was used as the loading control.

4.2.2 Liver-specific FoxO3 overexpression after birth leads to impaired growth

In our mouse model, FoxO3 overexpression was controlled through administration or deprivation of DOX dissolved in water. We switched on FoxO3 overexpression immediately after the mice were born by stopping DOX supplication, and analyzed the mice when they were 5 weeks old (Figure 5A).

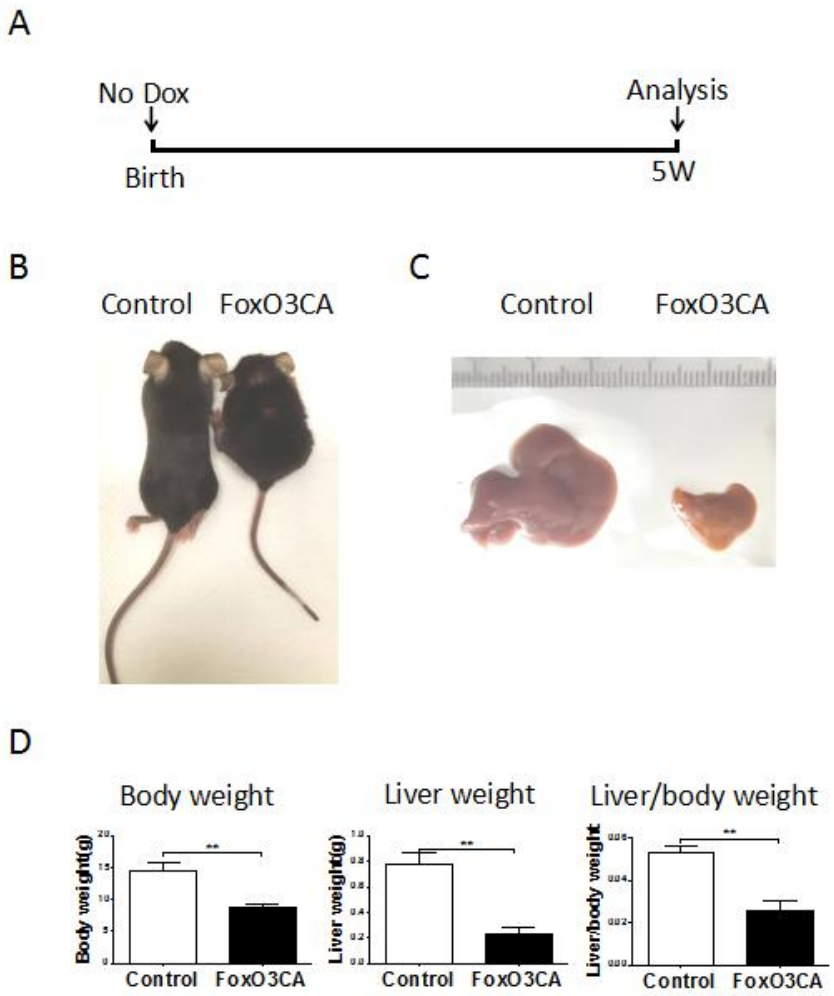

Figure 5. Liver-specific FoxO3 overexpression after birth leads to impaired growth

A. Schedule of DOX treatment. DOX water was abolished once the mice were born. The mice were analyzed when they were 5 weeks old.

B. Appearance of the FoxO3CA mice and WT mice.

C. Livers from the FoxO3CA and WT mice.

D. The body and liver weights of FoxO3CA mice (n = 4) and WT (n = 4) mice were measured, and their liver/body weight ratios were calculated. The p-values were analyzed using Student's t-test; ** $p < 0.01$.

The FoxO3CA mice were obviously smaller than the wild-type mice (Figure 5B). Meanwhile, the livers of the FoxO3CA mice were also much smaller than those of the wild-type mice (Figure 5C). The body and liver weight of both groups of mice were measured; both the body weights and liver weights of the FoxO3CA mice were significantly lower than those of the WT mice. In addition, the liver/body weight ratio was also lower in FoxO3CA mice, which indicates that the reduction in liver weight was more serious than the reduction in body weight (Figure 5D).

4.2.3 Liver-specific FoxO3 overexpression after birth leads to liver damage and impaired liver function

Since the reduction in liver weight was more serious than the reduction in body weight, liver damage was highly suspected in the FoxO3CA mice. Thus, several widely used liver damage markers such as serum alanine aminotransferase (ALT), aspartate aminotransferase (AST) and bilirubin tests were performed to identify the status of the livers. All of these markers were significantly elevated in the FoxO3CA mice (Figure 6A-C), indicating liver damage in the FoxO3CA mice.

Metabolic indicators such as blood glucose, serum cholesterol and triglyceride were also measured (Figure 6E, 6F). Neither cholesterol nor triglyceride showed significant differences between the wild-type and FoxO3CA groups. Meanwhile, the FoxO3CA group had lower blood glucose levels (Figure 6D). As known, FoxO family genes are transcription factors in the insulin-signaling pathway. The upregulation of FoxO proteins usually leads to hyperglycemia (92). This contrasts with our results, indicating that other unexpected signaling pathways may be activated in our FoxO3CA mice. In addition, the hepatic functional alteration induced by FoxO3 overexpression would be lethal to neonatal mice.

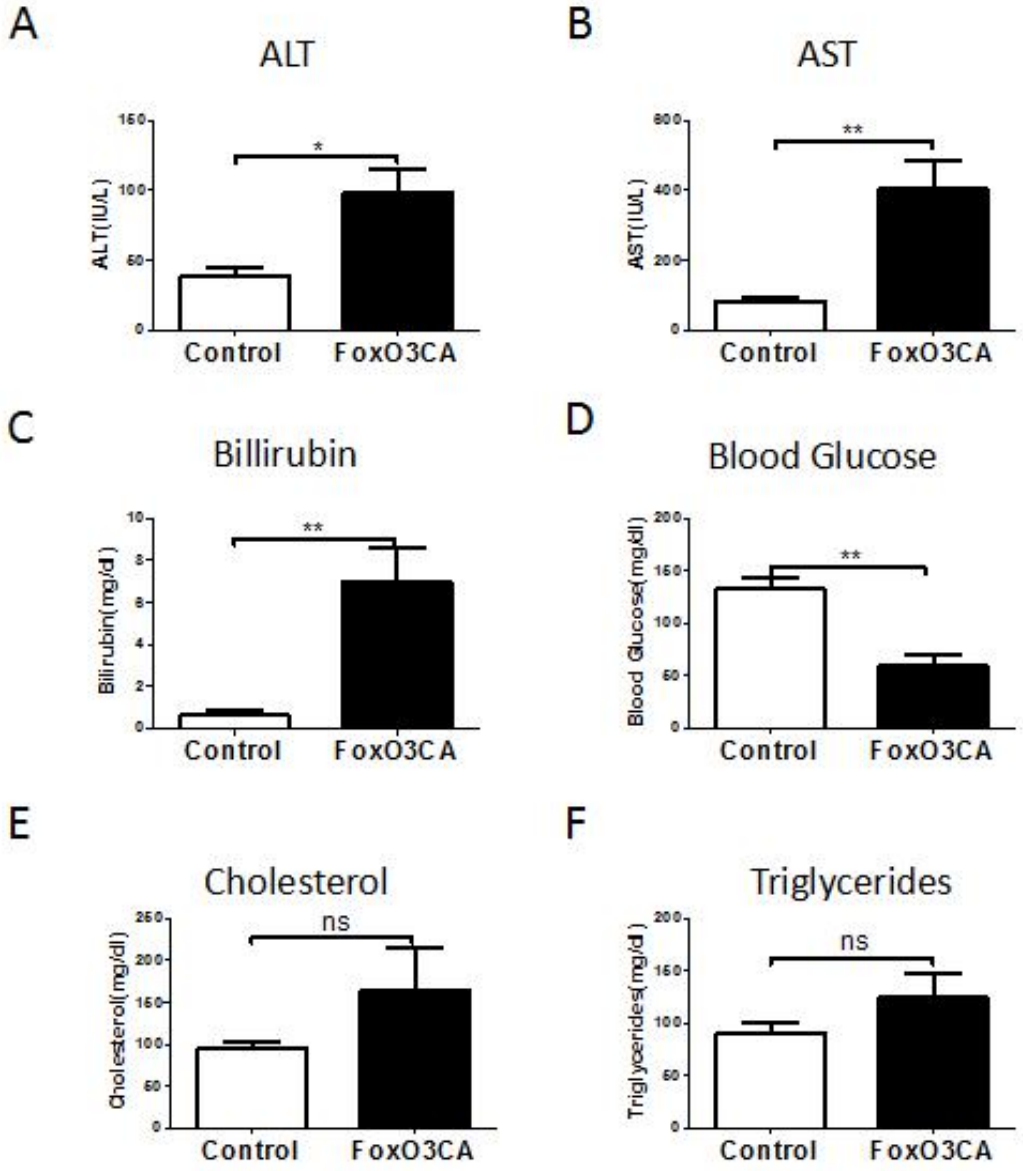

Figure 6. Liver-specific FoxO3 overexpression after birth leads to liver damage and impaired liver function

Alanine aminotransferase (ALT), **B.** aspartate aminotransferase (AST) and **C.** bilirubin levels in serum were measured. **D.** Blood glucose level, **E.** cholesterol and **F.** triglyceride were also tested in wild-type mice and FoxO3CA mice (n = 4); ns = not significant.

4.2.4 FoxO3 overexpression 5 weeks postoperatively leads to hyperglycemia

Hepatic FoxO3 overexpression after birth leads to severe liver damage and the impaired growth in the mice. I switched on FoxO3 overexpression when the mice were 5 weeks old, and the FoxO3CA mice and wild-type mice were

sacrificed and analyzed when they were 9 weeks old (Figure 7A). No significant difference were observed in their body weights, liver weights and liver/body weight ratios (Figure 7B), indicating that FoxO3 overexpression at a later time point might not induce obvious harm to the mice. In addition, the blood glucose level was significantly higher in FoxO3CA mice after 6 hours of fasting (Figure 7C, D). Hyperglycemia was induced by FoxO3 overexpression in hepatocytes.

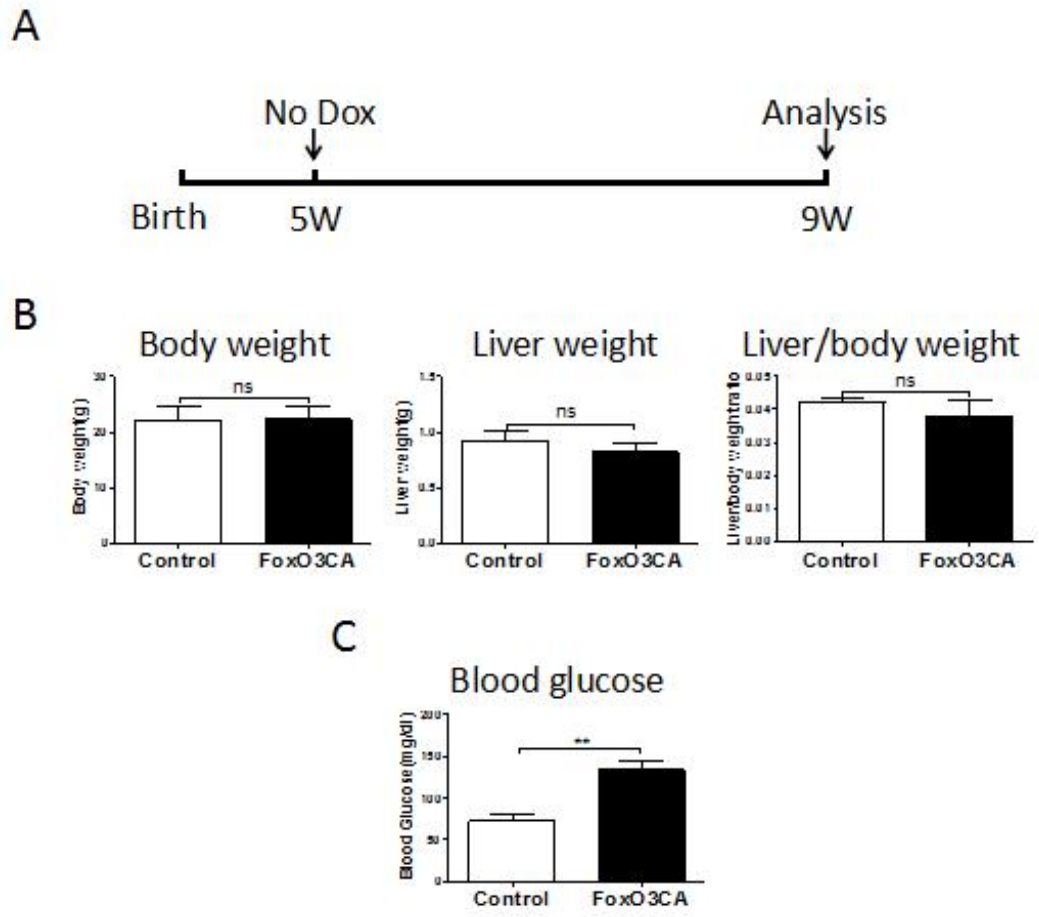

Figure 7. FoxO3 overexpression since 5 weeks old lead to hyperglycemia

A. Schedule of DOX treatment. DOX water was administrated until 5 weeks old. Mice were analyzed when they were 9 weeks old.

B. The body weight and liver weight of the FoxO3CA and WT groups (n = 4) were measured, and their liver/body weight ratios were calculated. Student's t-test showed $p > 0.05$.

C. Blood glucose level was measured after 6 hours of fasting. The p value was calculated using Student's t-test. ** $p < 0.01$; ns = not significant.

4.2.5 FoxO3 overexpression in hepatocytes leads to morphologic alterations

Alanine aminotransferase and aspartate aminotransferase were elevated in FoxO3CA mice, compared to wild-type mice. I performed HE staining on FoxO3CA mice to check their liver cells and structures.

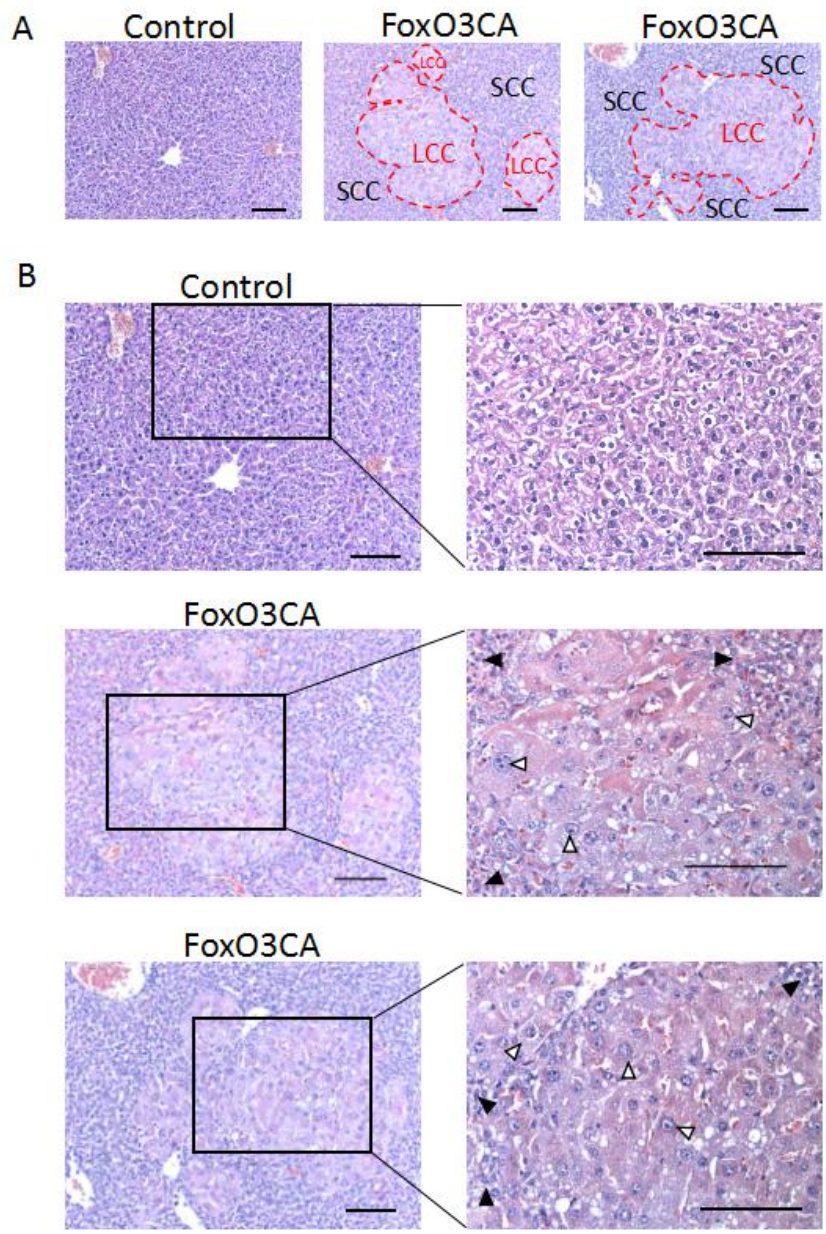

Figure 8. LCC and SCC lesions in FoxO3CA liver

A. HE staining on liver sections from wild-type mice and FoxO3CA mice.
Large cell change (LCC) and small cell change (SCC) were found in the FoxO3CA mouse livers. LCC cells were marked with white arrowheads, and SCC cells were marked with black arrowheads (scale bar: 100 μm).

Some hepatocytes were enlarged, with a normal nucleus/cytoplasm ratio, which is called large cell change (LCC). These enlarged hepatocytes gathered together to become LCC foci. However, the other hepatocytes around the LCC cells showed decreased cell volume, along with increased nucleus-to-cytoplasm ratio (Figure 8A, B), which is defined as small cell change (SCC). Both LCC and SCC were regarded as precursor lesions of HCC. LCC and SCC being identified in liver biopsies was thought to result in an increased risk of HCC over time (93)

4.2.6 FoxO3 overexpression induces elevated expression level of tumor-related genes

Since precancerous LCC and SCC lesions were observed in FoxO3CA mouse model, it is highly suspected that FoxO3CA leads to great potential for tumors at a later time. Thus, the expression levels of several tumor-related genes, including p53, H19, c-Myc, Kras, Pten Gpc3 and Perp, were determined by real-time PCR.

p53 is a tumor suppressor that is frequently mutated and upregulated in HCC (94). The non-coding RNA H19 is important for human tumor growth and could be a diagnosis and treatment target. H19 was upregulated in human HCC samples, and knockdown H19 in a HCC cell line impaired the growth of the cells (95). Additionally, 70% viral and alcohol-related HCC were found to have overexpressed c-Myc (96). Kras was reported as an oncogene that could promote HCC initiation and progression, when accompanied by HBV X protein(97). Pten works as a tumor suppressor by inhibiting the PI3K/AKT signaling pathway. Glypican-3 (GPC3) is a potential biomarker for early-stage HCC because it is expressed in HCC but not in benign liver tissues(98). Perp is a p53-associated gene that plays a role in tumor suppression.

As a result, p53, Pten and Kras were significantly elevated in the FoxO3CA mice compared to the WT mice (Figure 9A, D, F). Expression of the other

markers was also slightly increased, but the differences were not significant (Figures 9B, C, E, G, H).

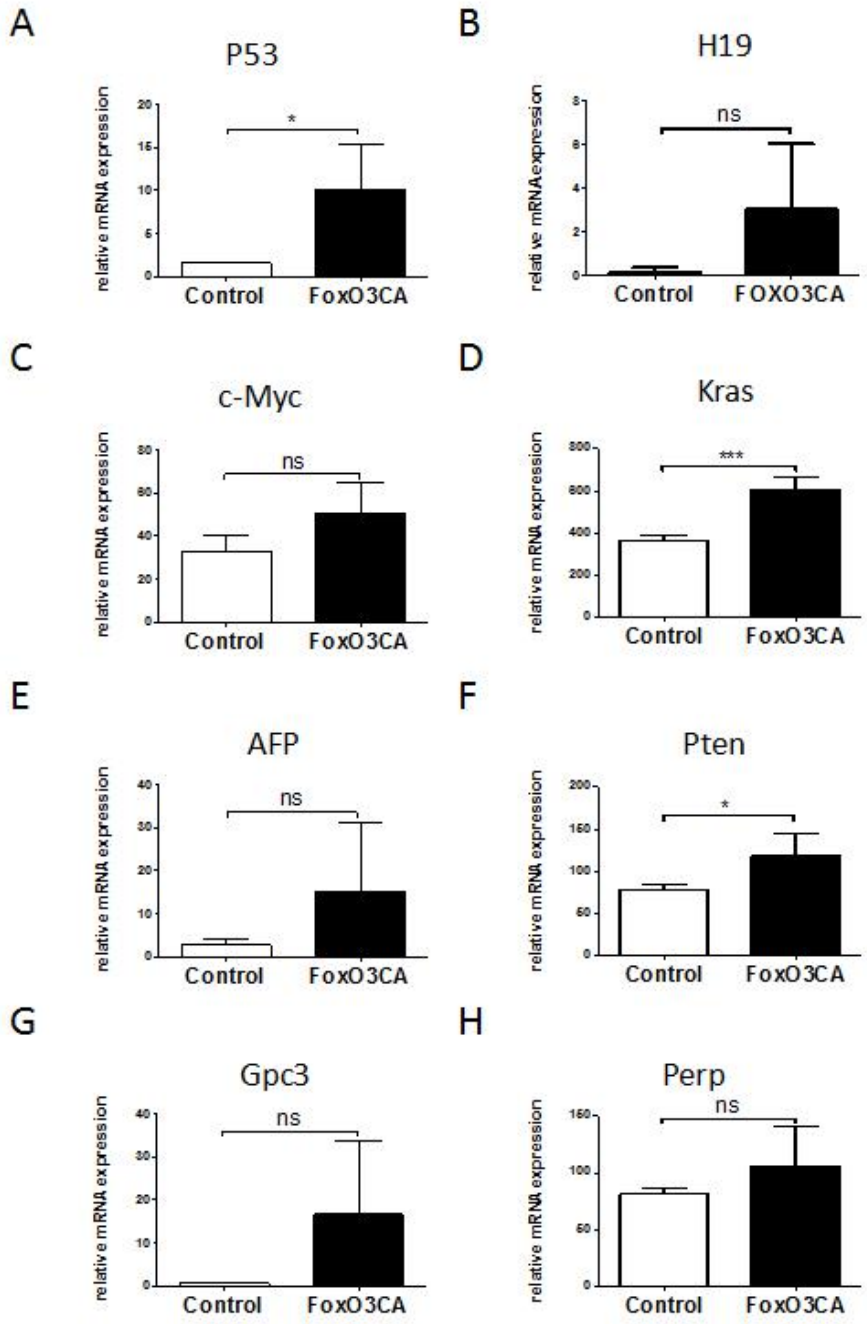

Figure 9. FoxO3 overexpression induce elevated expression level of tumor-related genes

The expression of tumor-related genes such as **A.** p53, **B.** H19, **C.** c-Myc, **D.** Kras, **E.** AFP, **F.** Pten, **G.** Gpc3 and **H.** Perp in the WT group (n = 4) and FoxO3CA group (n = 6) were measured by real-time PCR. The mRNA levels of these markers were normalized to the housekeeping gene GAPDH. P values were calculated using Student's t-test. * $p < 0.05$, ** $p < 0.01$,*** $p < 0.001$; ns = not significant.

4.2.7 FoxO3 is expressed in SCC cells

LCC and SCC lesions were found in the FoxO3CA livers, and it was unknown whether FoxO3 was expressed in both types of lesions. Hence, immunohistochemistry stain of FoxO3 was performed on sections from wild-type mice and FoxO3 mice. FoxO3 was expressed in the SCC areas but not in the LCC areas (Figure 10).

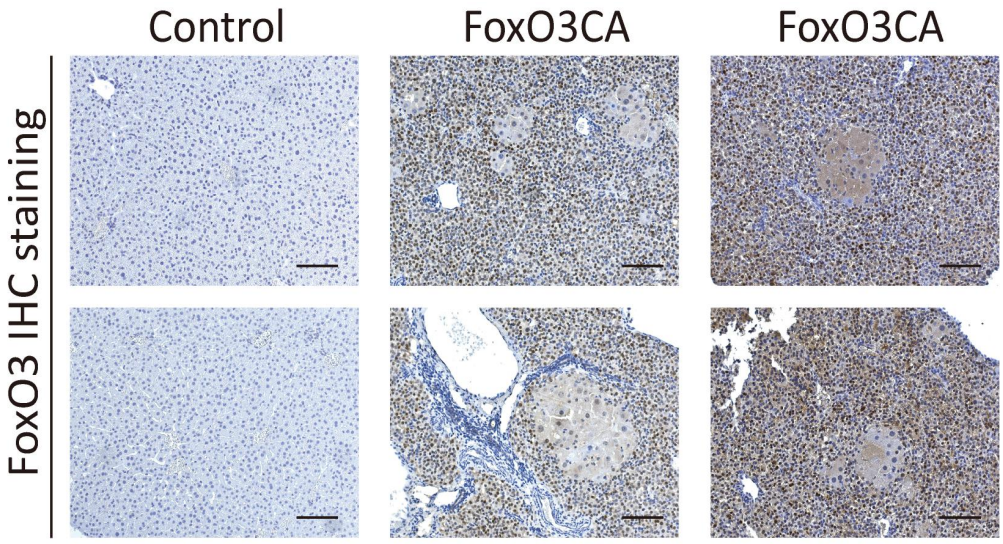

Figure 10. FoxO3 is expressed in SCC cells
Immunohistochemistry staining of FoxO3 was performed on WT and FoxO3 liver sections. FoxO3 was only stained in SCC cells (scale bar: 100 μm).

4.2.8 Akt is strongly phosphorylated in SCC cells

FoxO3 protein is regulated by the PI3K/AKT signaling pathway. Activated Akt can inhibit the activity of FoxO3 protein and translocate it out of the nucleus. I conducted Akt phosphorylation on mutated FoxO3 alleles to achieve a constitutive active form of FoxO3. However, FoxO3 overexpression was lost in the hepatocytes in the LCC areas. To determine whether FoxO3 in LCC cells is inhibited by Akt, IHC staining of Phospho-Akt was performed on the FoxO3CA

and WT groups. Astonishingly, p-Akt was absent in the WT sections and LCC cells but expressed in the SCC cells (Figure 11A). Western blot was also used to measure the expression level of p-Akt in the WT and FoxO3CA mice. P-Akt protein was upregulated in FoxO3CA mice (Figure 11B). These results imply that FoxO3 overexpression lead to Akt activation in hepatocytes possibly by a feedback mechanism.

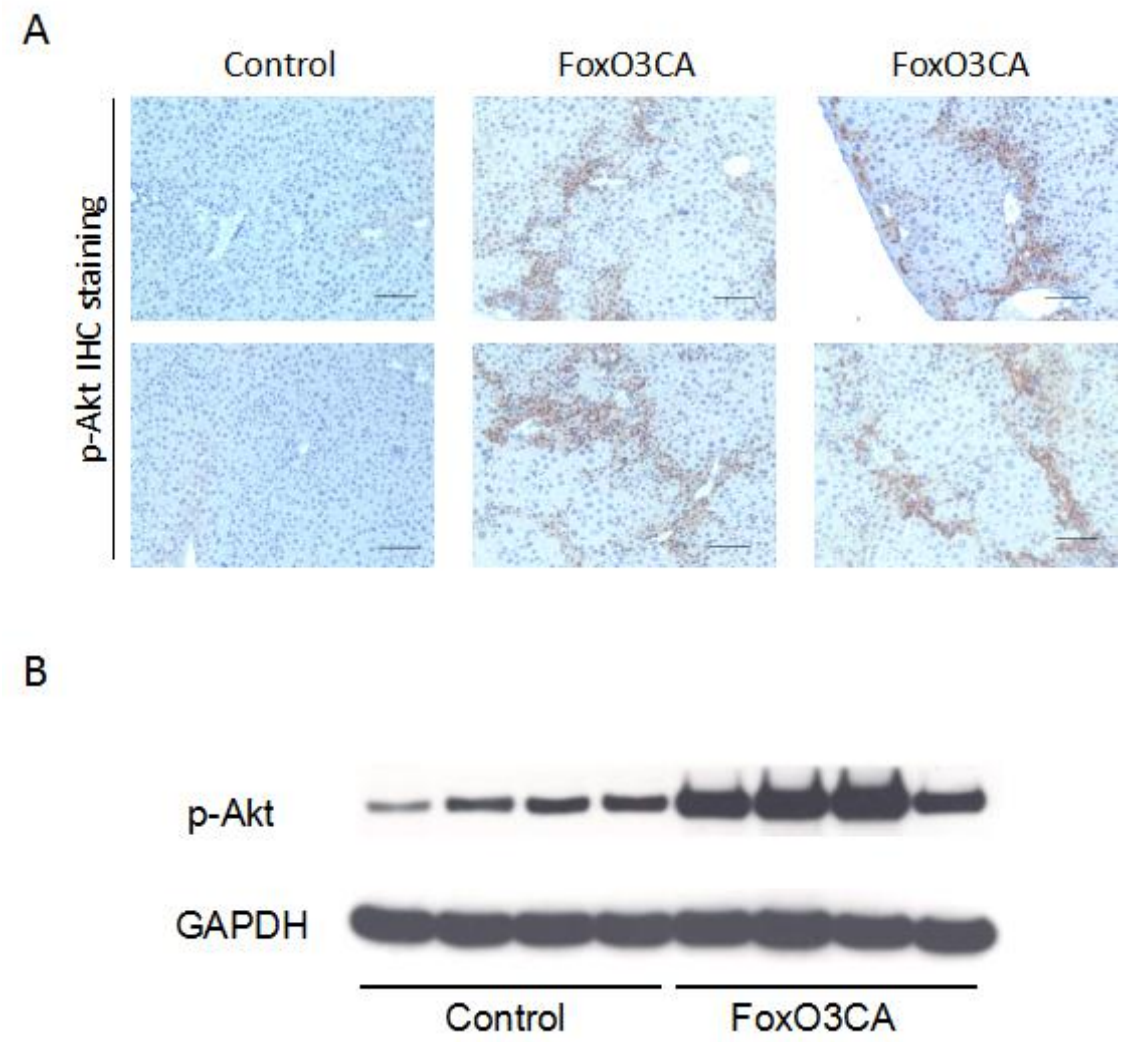

Figure 11. Phospho-Akt is upregulated in SCC cells

A. IHC staining of p-Akt on WT and FoxO3CA liver sections (scale bar: 100 μm).

B. Western blot analysis of p-Akt and GAPDH in the WT and FoxO3CA mice. GAPDH was used as the loading control.

4.2.9 Oval cells are not activated in FoxO3CA mice

From FoxO3 IHC staining, we found that hepatocytes in the LCC area did not express FoxO3 in our FoxO3CA mice. I am curious about where these expanded LCC cells came from.

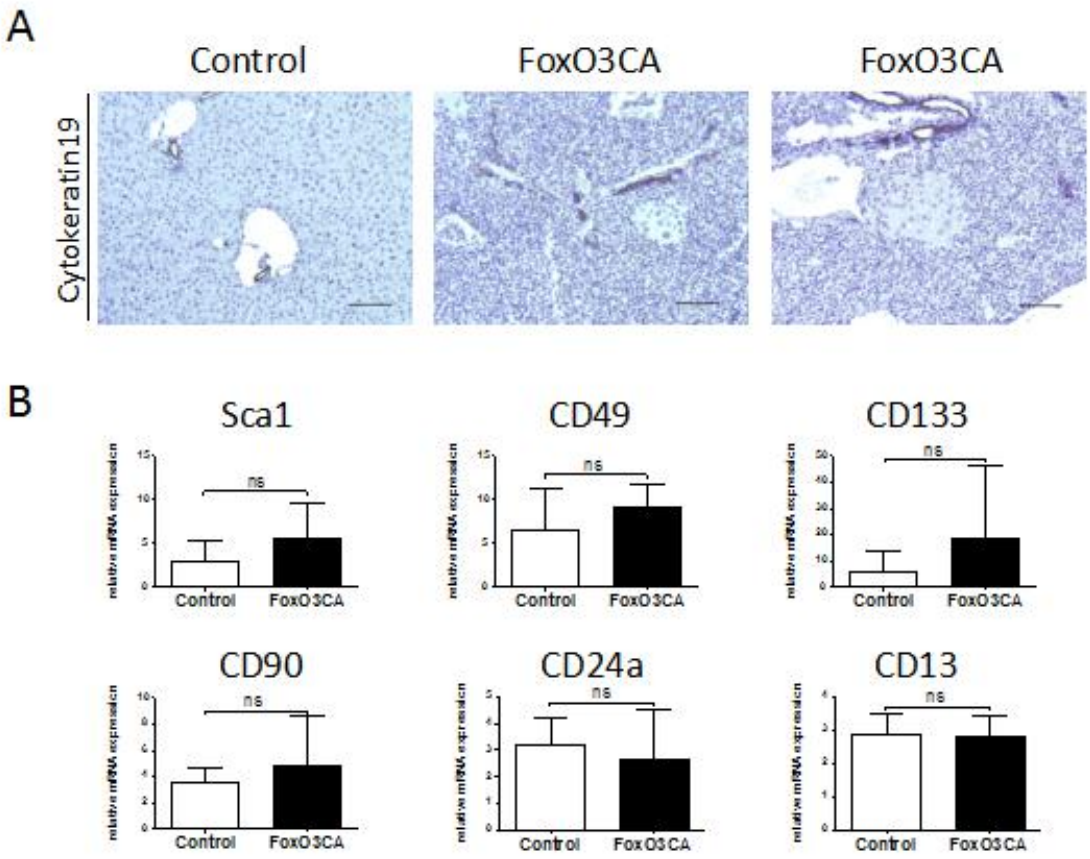

Figure 12. Oval cells are not activated in FoxO3CA mice

A. IHC staining of cytokeratin 19 was performed in the FoxO3CA and WT mice (scale bar: 100 μm).

B. Real-time PCR analysis of stem cell markers Sca1, CD49, CD133, CD90, CD24a and CD13. The results were normalized to housekeeping gene GAPDH. Student's t-test was performed. No significant statistical differences were observed; ns = not significant.

They proliferated from matured FoxO3 negative hepatocytes that escaped from the tet-off system or from activated hepatic oval cells. Severe hepatic damage induced by chemical toxicants, viruses, genome modifications or partial hepatectomy can lead to the activation of hepatic oval cells to

compensate for impaired liver function (99). Hepatic oval cells exhibit both types of epithelial cells—hepatocytes and cholangiocytes—in the liver (100). Thus, oval cell activation is usually accompanied with bile duct reaction. Hence, we performed IHC staining of cytokeratin 19 (CK19), which is a marker of cholangiocytes. Bile duct reactions were not observed in the FoxO3CA mice (Figure12 A). In addition, the mRNA level of stem cell markers such as Sca1, CD49, CD133, CD90, CD24a and CD13 were quantified with real-time PCR, and none of them were elevated in the FoxO3CA group (Figure12 B). These results indicate that oval cells were not activated in the FoxO3CA mice.

4.2.10 Proliferation is impaired in both LCC and SCC areas

LCC and SCC lesions were observed in the FoxO3CA mice, whether FoxO3 was overexpressed after birth or at 5 weeks old. The proliferation rates of LCC and SCC were determined by IHC staining of proliferate markers such as KI67 and PH3. KI67 protein is strictly associated with cell proliferation, because it is expressed in all active phases of the cell cycle (G1, S, G2 and mitosis) but not in the G0 phase (101). On the contrary, phosphorylated histone H3 (pH3) was specifically expressed in the mitosis phase (102). KI67 was stained in the LCC cells but absent in the SCC cells. The percentage of KI67-positive hepatocytes in the FoxO3CA mice showed no significant difference compared with that of the WT mice (Figure 13A, B). PH3 was also not stained in the SCC cells. Additionally, the LCC area had much less PH3-stained hepatocytes than the WT mice (Figure 13A, C).

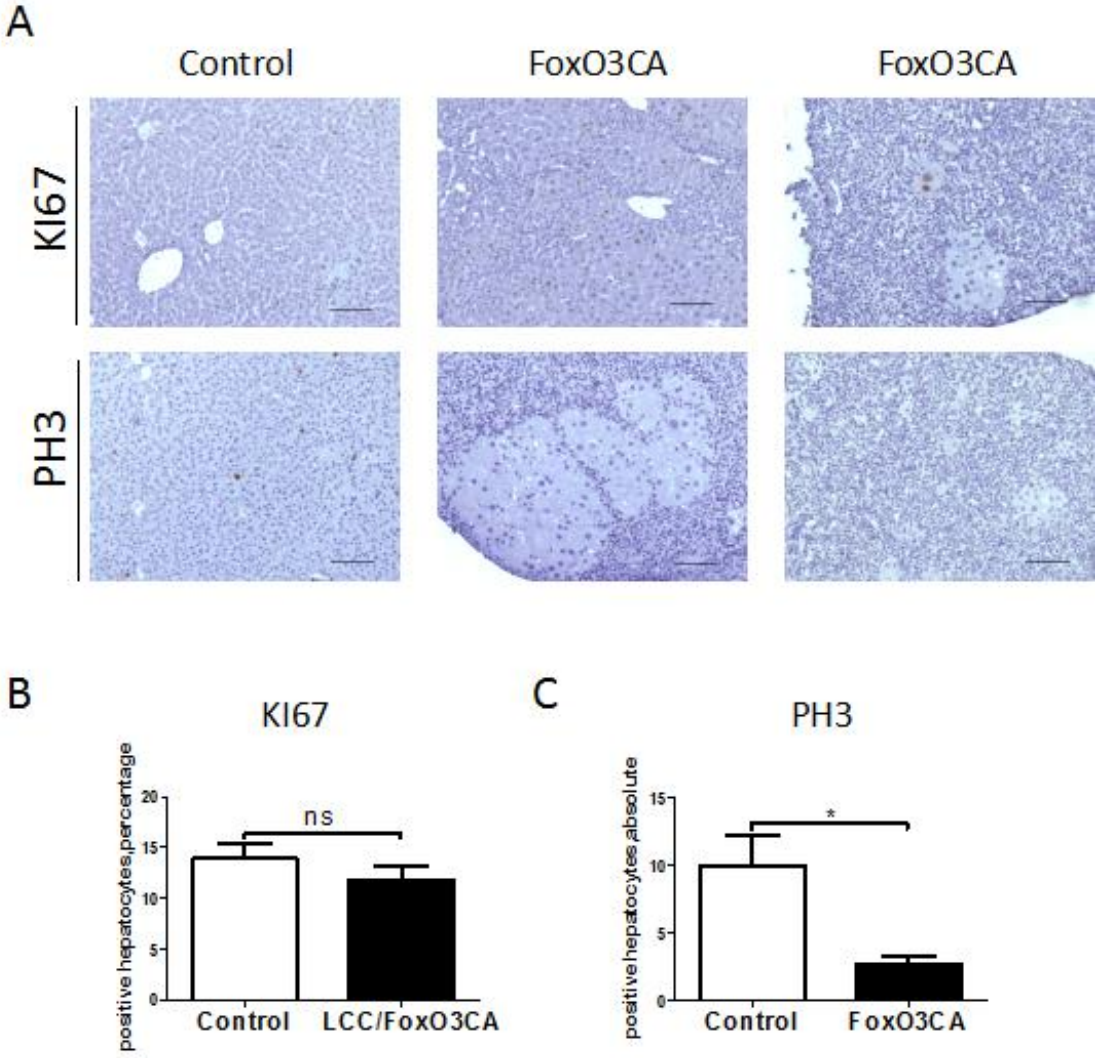

Figure 13. Proliferation is impaired in both LCC and SCC cells

A. Proliferation markers KI67 and PH3 were determined by IHC staining (scale bar: 100 μm).

B. Percentage of positive KI67 hepatocytes in the FoxO3CA mice, which were counted and analyzed. Student's t-test showed no significant differences.

C. Positive PH3 hepatocytes were counted. The p values were calculated using Student's t-test. * $p < 0.05$; ns = not significant.

4.2.11 p53-p21 pathway is activated in LCC cells

The hepatocytes in the LCC areas proliferated very slowly compared with those in the WT mice. Decreased proliferation of cells in the mitosis phase, indicating cell cycle arrest, existed in the LCC areas. In addition, enlarged cellular size also indicates cell cycle issues. p53, a tumor suppressor, is also a

critical transcription factor for cell cycle arrest. p53 can arrest the cell cycle's progression by inducing the expression of p21, an inhibitor of cyclin-dependent kinases (103). Thus, p53 and p21 expression were checked by IHC staining. The results showed that both p53 and p21 were stained in the LCC cells (Figure 14A, B).

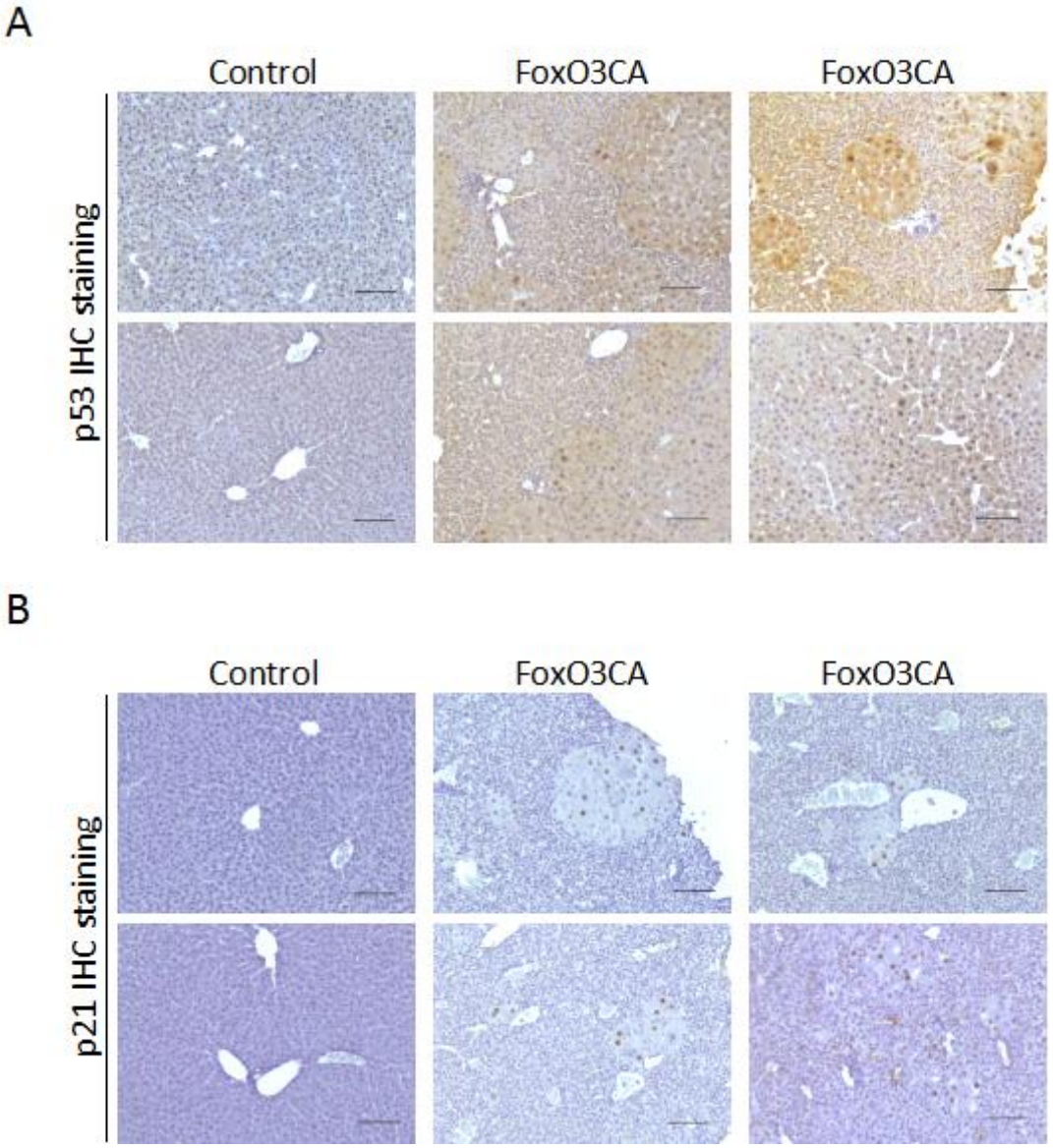

Figure 14. p53 and p21 pathway was activated in LCC cells
IHC staining of **A.** p53 and **B.** p21 in the FoxO3CA mice and the WT mice (scale bar: 100 μm).

4.2.12 FoxO3 activation in SCC areas leads to the expression of markers for DNA damage and HCC

Small cell change and large cell change have been considered as potential lesions of hepatocellular carcinoma. The mRNA levels of HCC-related genes such as p53, Pten and Kras were elevated in the FoxO3CA mice. Both SCC and LCC lesions existed in our FoxO3CA mouse model. Which of these two types of lesions was more malignant still needs to be determined. Markers for DNA damage and HCC progression, including 8-OHdG, AFP and γH2AX, were checked by IHC staining. All of these markers were stained in the SCC areas, indicating that the SCC lesions were more advanced precancerous lesions than the LCC lesions (Figure 15).

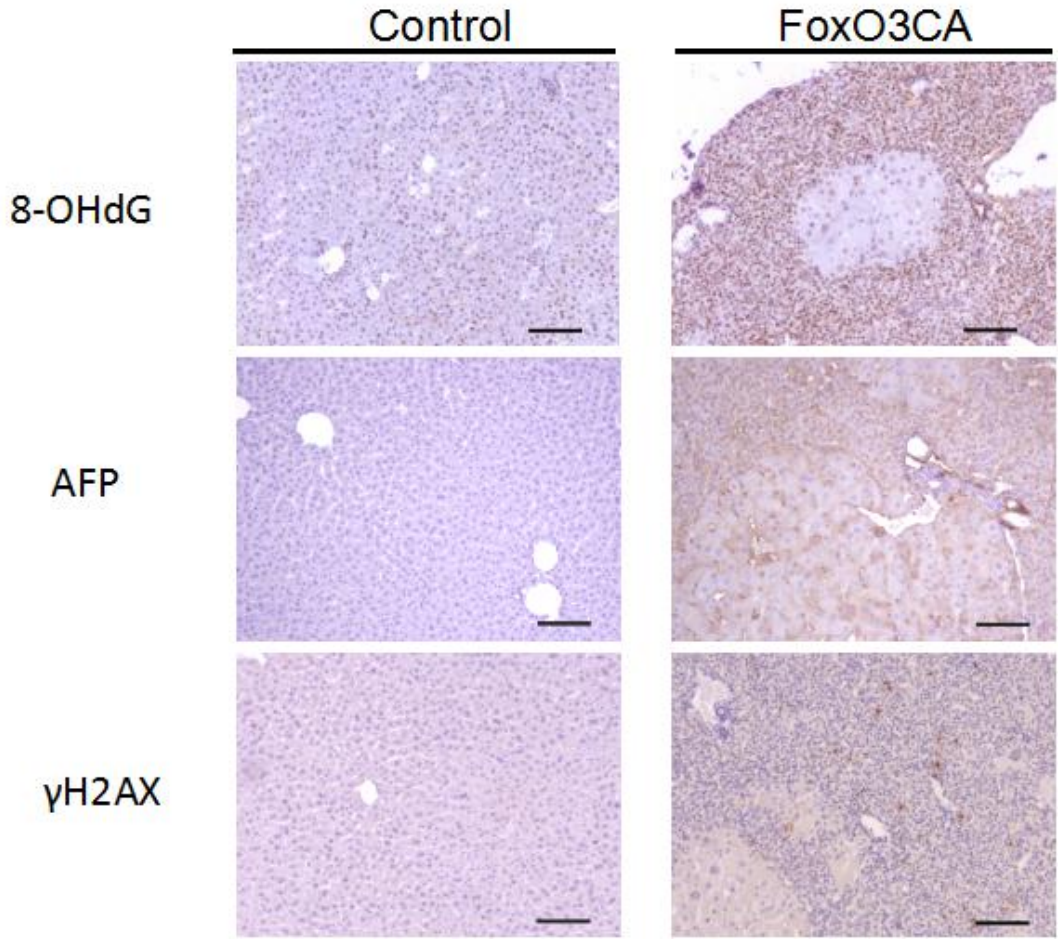

Figure 15. Markers for DNA damage and HCC were expressed in the SCC areas
IHC staining of 8-OHdG, AFP and γH2AX in the FoxO3CA mice and WT mice (scale bar: 100 μm).

Alpha-fetoprotein (AFP) is an oncofetal protein expressed in fetal gut and liver. It is not expressed in normal liver but expressed in HCC. Hence, it has been widely used as a biomarker for HCC.

4.2.13 Hepatic FoxO3 overexpression leads to faster tumorigenesis after DEN injection

DNA damage existed in the SCC areas, which may have caused hepatocarcinogenesis due to increased risk for genomic alterations. Thus, DEN injection was performed on the FoxO3CA and WT mice when they were 15 days old. DOX water were deprived at 5 weeks after birth, and the mice were analyzed at 10 months old (Figure 16A). MRI scanning showed that the FoxO3CA mice had more tumors than the mice in the WT group (Figure 16B). All 6 mice in the FoxO3CA group had tumors 10 months after DEN injection, whereas only 2 out of the 7 WT mice had tumor generation. Tumor formation induced by DEN in the FoxO3CA mice occurred significantly faster than in the WT mice (Figure 16C). The numbers of tumors in the FoxO3CA and WT mice were counted, and the FoxO3CA mice had many more tumors than the WT mice (Figure 16D). The mice were sacrificed when they were around 11 months old. The tumorigenesis in the FoxO3CA mice looked much more severe than in the WT mice (Figure 16E). The body weights of the FoxO3CA and WT mice showed no significant differences (Figure 16F). However, the FoxO3CA mice had significantly higher liver weights and liver/body weight ratios (Figures 16G, H). There results implied that the FoxO3CA mice had more tumors than the WT mice.

A

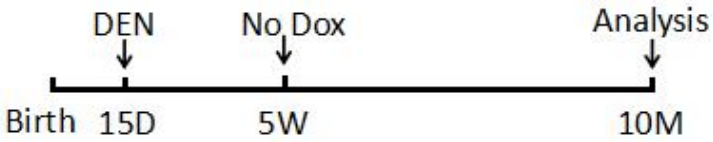
DEN
No Dox
Analysis
Birth
15D
5W
10M

B

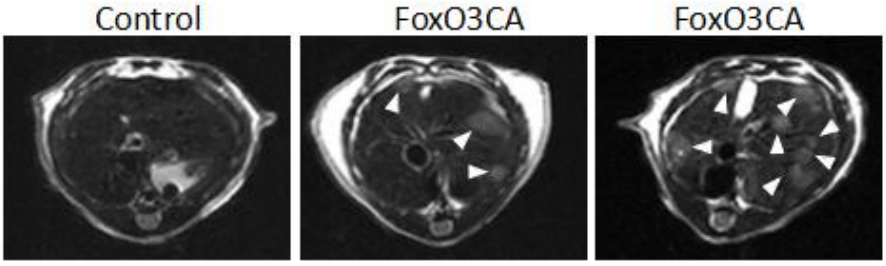
Control
FoxO3CA
FoxO3CA

C

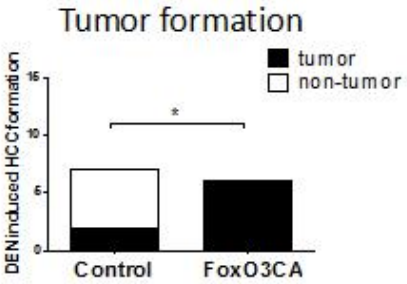
Tumor formation
tumor
non-tumor
DEN induced HCC formation
*
Control
FoxO3CA

D

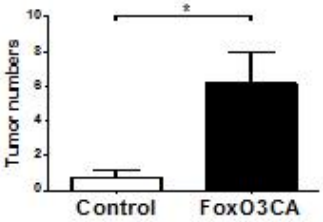
Tumor numbers
*
Control
FoxO3CA

E

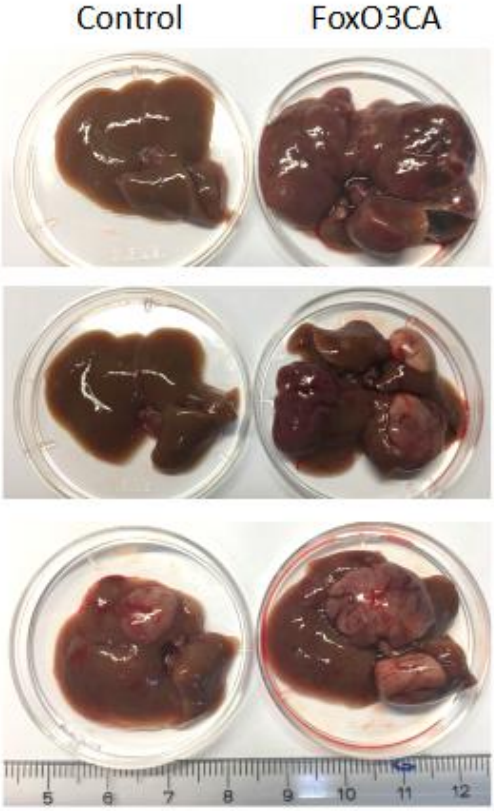
Control
FoxO3CA

F

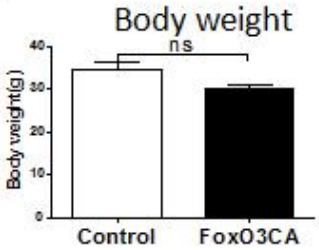
Body weight
ns
Body weight(g)
Control
FoxO3CA

G

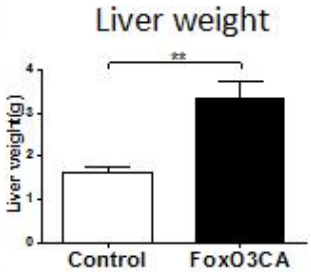
Liver weight
**
Liver weight(g)
Control
FoxO3CA

H

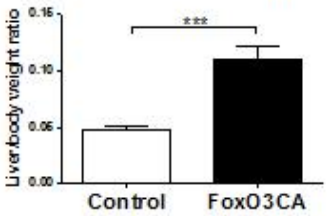
Liver/body weight
***
Liver/body weight ratio
Control
FoxO3CA

Figure 16. Hepatic FoxO3 overexpression leads to enhanced tumorigenesis after DEN injection

A. Schedule of DEN injection and DOX administration. DEN injection was performed 15 days after birth, and DOX water was deprived 5 weeks after birth.

B. MRI scanning was performed 10 months after birth. The tumors are marked with white arrowheads.

C. The mice were divided into tumor and non-tumor groups according to MRI scanning. The p values were calculated using Fisher's exact test. * $p < 0.05$.

D. The number of tumors in each mouse was counted according to MRI scanning. The p values were calculated using Student's t-test. * $p < 0.05$.

E. Livers from the FoxO3CA and WT mice 11 months after DEN injection.

F. Body weight of the FoxO3CA and WT mice. Student's t-test showed no statistical differences; ns = not significant.

G. Liver weight of the FoxO3CA and WT mice. The p values were analyzed using Student's t-test. ** $p < 0.01$.

Liver/body weight ratios. The p values were analyzed using Student's t-test. *** $p < 0.001$.

5. DISCUSSION

5.1 Controversial views on the role of FoxO3 in tumorigenesis

The role of FoxO family transcription factors have gained more and more attention in recent years because they are involved in multiple cellular activities, such as glucose and lipid metabolism, proliferation and cell cycle arrest, resistance to oxidative stress, apoptosis and atrophy. Some members of the FOXO family were even initially found at chromosomal translocations in human tumors (104, 105). FOXO3 was discovered as a fusion partner with the mixed-lineage leukemia gene in acute myeloid leukemia (104). Since FoxO proteins exhibit so many cellular activities and they could be the key factor to determine the fate of malignant or precancerous cells, we are very interested in what kind of role FoxO3 plays in the development of hepatocellular carcinoma.

The role of FoxO3 in HCC is still controversial. Several studies from the literature have tried to illustrate the relation between HCC and FoxO3, and the researchers hold different opinions. On one hand, it has been demonstrated that FoxO3 acts as a tumor suppressor because it can induce cell cycle arrest by activating cell cycle arrest-related genes. For example, FoxO3 activation induced by the TNF superfamily ligand APRIL could trigger cell cycle arrest in HepG2 and Hep3B cell lines by upregulating GADD45 (106). Additionally, when FoxO3 is upregulated by melatonin treatment, it can cause apoptosis in HepG2 cell lines by expressing the downstream target Bim (107). On the other hand, some studies suggest that FoxO3 could act as a tumor supporter. For example, FoxO3 could promote the survival of cancer cells under stress conditions, such as doxorubicin treatment and hypoxia (108). All in all, these studies are not convincing because they are all *in vitro* studies. Since FoxO3 is a transcription factor that is involved in multiple functions, it can perform different activities, depending on the cell type and cell environment. FoxO3

activation and upregulation induced by drug treatment or upstream regulators could lead to a fake effect because other factors and signaling pathways could also be activated. Thus, we used a hepatic constitutive FoxO3 overexpression mouse model to study the role that FoxO3 plays in HCC genesis.

5.2 FoxO3 activation impairs hepatocyte differentiation and liver growth

My mouse model is conditional hepatic FoxO3 overexpression model. The expression of FoxO3 in hepatocytes can be controlled by doxycycline. When overexpressed FoxO3 was switched on immediately after birth, the growth and development of the mice was impaired. Liver damage was observed in the FoxO3CA mice. Thus, we assumed that FoxO3 overexpression affects the proliferation and differentiation of hepatocytes in immature mice. Even though how FoxO3 regulates the cellular differentiation of hepatocytes has not been reported, FoxO3 was found to exhibit an anti-differentiation effect in other organs, such as in female gonads. FoxO works at the earliest stage of follicular growth as a suppressor of follicular activation (109). Also, constitutively active FoxO1 prevents the differentiation of preadipocytes, while dominant-negative FoxO1 rescues adipocyte differentiation in insulin receptor-deficient mice (110). In addition, FoxO transcription factors also play a role in differentiating myoblasts and pancreatic β cells (111, 112). Hence, FoxO3 could also play a role in differentiating hepatocytes, but the mechanism behind it remains unknown. The main aim of this study is to determine the role that FoxO3 plays in HCC genesis. We decided to switch on FoxO3 overexpression at a later time point: at the age of 5 weeks old. No liver damage or impaired growth was observed.

5.3 Precancerous lesions LCC and SCC induced by FoxO3 over-expression

The FoxO3 overexpression mouse model was confirmed by both western blotting and IHC staining. FoxO3 protein was increased in the FoxO3CA mice, and FoxO3 was stained in nuclei of the mice. However, HE staining showed morphological changes in the hepatocytes of mice with FoxO3 over-expressed from birth and at 5 weeks old. These morphological changes are in accord with so-called large cell change (LCC) and small cell change (SCC) in the literature. Both LCC and SCC were considered to represent potential precursor lesions of hepatocellular carcinoma (HCC). Compared to LCC, SCC were thought to be precancerous lesions because DNA damage marker gammaH2AX was highly expressed in SCC areas but not in LCC areas, whereas p21 was highly expressed in LCC areas and reduced in SCC and HCC areas (113). My results coincided with these views. First, the p53-p21 signaling pathway was activated only in LCC areas. Second, in the FoxO3CA mice, gammaH2AX was highly expressed in SCC areas. In addition, a marker of oxidative stress, 8-OHdG, was also found to be expressed in SCC areas, indicating that reactive oxygen species (ROS)-induced DNA damage existed in the SCC areas. All of these findings support that SCC is a more malignant lesion than LCC. Additionally, the mRNA levels of several HCC-related genes were found to be increased in the FoxO3CA group. Hence, FoxO3 has the potential to have HCC at a later time point.

I determined the proliferation rate of the FoxO3CA livers, because malignant lesions usually have strong proliferative ability. From the literature, SCC found in human sections showed as high of a proliferation rate as HCC, whereas LCC showed a reduced proliferative ability (114). However, some researchers also claim that most preneoplastic lesions are quiescent and do not progress to form tumors (115). However, proliferation in SCC areas was impaired and

LCC was still proliferating in our mouse model. Hence, LCC and SCC lesions in our mouse model are different from the lesions found in human tissue. Then, we checked the expression of FoxO3 in the FoxO3CA mice by IHC staining. FoxO3 is highly expressed in SCC areas but suppressed in LCC. Hence, in summary, SCC cells were FoxO3 positive with increased ROS and DNA damage as well as impaired proliferation. LCC cells were FoxO3 negative with activated p53-p21 pathway.

5.4 Oval cells are not activated in FoxO3CA mice

Severe liver damage induced by viruses, chemicals or transgenetics can activate oval cells to restore the liver function (116). For example, active Wnt/beta-Catenin signaling contributes to oval cell activation (117). In addition, hepatic oval cell activation could secure genetic modification-induced liver damage by generating healthy hepatocytes. In the conditional survivin knockout model, liver damage induced the activation of oval cells, and newly generated hepatocytes retained survivin expression (118). Thus, we were very interested about whether oval cells were activated in our mouse model. If oval cells were activated in our mouse model, it could explain why FoxO3 was negatively regulated in LCC cells, since oval cells can be differentiated into both hepatocytes and cholangiocytes when they are activated. Oval cell activation is usually accompanied by the proliferation of cholangiocytes, which is also called bile duct reaction. We stained cholangiocyte marker cytokeratin 19 and used real-time PCR for several stem cell markers. The results suggest that FoxO overexpression did not trigger the activation of oval cells. Hence, hepatocytes overexpressing FoxO3 could be rescued, and the expression of FoxO3 was decreased by an unknown mechanism.

5.5 ROS and DNA damage are induced by FoxO3CA

ROS-induced DNA damage existed in the SCC cells. As mentioned above, DNA damage could trigger DNA damage response (DDR) pathways, including DNA repair, cell cycle arrest and in the end, cell death or senescence. The SCC cells with overexpressed FoxO3 were not undergoing apoptosis. On the other hand, the p53-p21 signaling pathway was activated in the LCC cells. The tumor suppresser p53 was proven to be recruited in response to DNA damage and plays an important role in cell cycle regulation. The cyclin-dependent kinase inhibitor p21 is a direct downstream of p53. The activation of p53-p21 implies cell cycle arrest in LCC cells. This also explains the enlargement of the cell size. Cell cycle arrest offers cells time to repair the DNA damage. Once DNA damage is repaired, the cells with arrested cell cycles will resume cell cycle progression, and unrepaired cells will undergo permanent cell cycle arrest or apoptosis (119). Hence, it is possible that LCC cells come from cells that overexpress FoxO3. FoxO3 induces ROS and DNA damage in hepatocytes. Some of these DNA-damaged hepatocytes led to cell cycle arrest by activating the p53-p21 signaling pathway. Whereas other hepatocytes overexpressing FoxO3 retained DNA damage, they could survive and become malignant in the future.

However, we could not confirm how FoxO3 induces ROS and DNA damage in our mouse model. However, the literature suggests that ROS could be induced by FoxO3 target genes such as Bim and BclxL (120).

5.6 FoxO3 promotes tumorigenesis in DEN-injected mice

We kept the mice overexpressing FoxO3 until they were one year old, and they did not form tumors. We realized that FoxO3 overexpression was not sufficient to induce a tumor but that it could be able to enhance tumorigenesis under another trigger. Hence, we performed DEN injection on the FoxO3CA and WT

mice. We chose DEN because whether DEN induces HCC mainly depends on ROS and DNA damage, which coincides with FoxO3's effects in our mouse model. The results showed that the FoxO3CA mice had more and earlier HCC than the WT mice. The DEN-injected FoxO3CA mice had more tumorigenesis due to two possible reasons. First, the FoxO3CA mice had more ROS and DNA damage because they already had FoxO3 overexpression induced in them. Second, FoxO3 activation can keep cells alive under stress conditions, such as ROS and DNA damage. FoxO3 can protect cells from ROS-induced damage and apoptosis by activating detoxifying enzymes such as catalase and sestrins, and by reducing mitochondrial mass and oxygen consumption (121). Additionally, long-term DNA damage would promote the development of HCC.

5.7 The expression of FoxO3 in human samples

We checked the expression level of FoxO3 in human tissues. The FoxO3 staining showed that FoxO3 was activated in 48.4% of human sections, whereas the mRNA levels of FoxO3 determined by real-time PCR showed that FoxO3 mRNA was not upregulated, compared to in healthy livers. FoxO3 is a transcription factor that is activated in the nucleus and inactivated in cytoplasm. FoxO3 was observed to be expressed and activated in some of the HCC patients. Even though the mRNA levels of FoxO3 were not elevated in the HCC patients, FoxO3 was activated and exhibited transcriptional functions in the nucleus. Thus FoxO3 could be a potential biomarker and therapy target of HCC. In addition, our study suggests that FoxO3 promotes tumor cells being alive under oxidative stress, so FoxO3 positivity could be a signal suggesting insensitivity to treatment and poor outcomes.

5.8 Conclusion

In our study, we demonstrated the role of FoxO3 in HCC development using a hepatic, constitutively active FoxO3 overexpressing mouse model. FoxO3 overexpression after birth led to impaired growth and liver damage. However, the mice exhibited normal phenotype when FoxO3 was overexpressed since the mice were 5 weeks old. Precancerous lesions such as LCC and SCC were found in the FoxO3CA mice. The SCC cells were overexpressing FoxO3; meanwhile, ROS and DNA damage were found to exist in the SCC cells. FoxO3CA also enhanced DNA-induced HCC development. The mechanism could be that FoxO3 overexpression induces ROS accumulation in hepatocytes and inhibits ROS and DNA damage-induced cell apoptosis and death.

6. SUMMARY

FoxO3, a transcription factor of the Forkhead family, plays a role in multicellular activities such as glucose and lipid metabolism, proliferation and cell cycle arrest, resistance to oxidative stress, apoptosis and atrophy. We found that FoxO3 could be activated in human HCC samples. However, the role that FoxO3 plays in HCC is still unclear. FoxO3 was found to execute different functions under different treatment. Hence, we established an in vivo FoxO3 overexpression mouse model to clarify the role of FoxO3 in HCC development.

Hepatic, constitutively activated FoxO3 overexpression after birth led to severe liver damage. When FoxO3 overexpression was switched on at 5 week old, no obvious liver damage was observed, but we still observed morphological alterations such as precancerous LCC and SCC lesions. FoxO3 was expressed in SCC cells but absent in LCC cells. ROS and DNA damage existed in the SCC areas, and the p53-p21 signaling pathway was activated in LCC areas. ROS and DNA damage could be induced directly by FoxO3 activation. FoxO3 can protect cells from apoptosis and cell death under oxidative stress and DNA damage, which could lead to tumorigenesis.

We injected the FoxO3CA mice and WT mice with DEN. Ten months after the DEN injection, a greater proportion of the FoxO3CA mice had tumors than the WT mice. Also, the numbers of tumors among the FoxO3CA mice were much greater than those of the WT mice.

In conclusion, our study suggests that FoxO3 acts as an oncogene in HCC. FoxO3 could promote tumorigenesis by inhibiting the apoptosis and cell death of DNA-damaged hepatocytes.

7. REFERENCES

1. Racanelli V, Rehermann B. The liver as an immunological organ. *Hepatology* 2006; 43: S54-62.
2. Kaul VV, Munoz SJ. Coagulopathy of Liver Disease. *Current treatment options in gastroenterology* 2000; 3: 433-438.
3. Rappaport AM, Borowy ZJ, Lougheed WM, Lotto WN. Subdivision of hexagonal liver lobules into a structural and functional unit; role in hepatic physiology and pathology. *The Anatomical record* 1954; 119: 11-33.
4. Sasse D, Spornitz UM, Maly IP. Liver architecture. *Enzyme* 1992; 46: 8-32.
5. Jemal A, Bray F, Center MM, Ferlay J, Ward E, Forman D. Global cancer statistics. *CA: a cancer journal for clinicians* 2011; 61: 69-90.
6. Global Burden of Disease Cancer C, Fitzmaurice C, Dicker D, Pain A, Hamavid H, Moradi-Lakeh M, MacIntyre MF, Allen C, Hansen G, Woodbrook R, Wolfe C, Hamadeh RR, Moore A, Werdecker A, Gessner BD, Te Ao B, McMahon B, Karimkhani C, Yu C, Cooke GS, Schwebel DC, Carpenter DO, Pereira DM, Nash D, Kazi DS, De Leo D, Plass D, Ukwaja KN, Thurston GD, Yun Jin K, Simard EP, Mills E, Park EK, Catala-Lopez F, deVeber G, Gotay C, Khan G, Hosgood HD, 3rd, Santos IS, Leasher JL, Singh J, Leigh J, Jonas JB, Sanabria J, Beardsley J, Jacobsen KH, Takahashi K, Franklin RC, Ronfani L, Montico M, Naldi L, Tonelli M, Geleijnse J, Petzold M, Shrime MG, Younis M, Yonemoto N, Breitborde N, Yip P, Pourmalek F, Lotufo PA, Esteghamati A, Hankey GJ, Ali R, Lunevicius R, Malekzadeh R, Dellavalle R, Weintraub R, Lucas R, Hay R, Rojas-Rueda D, Westerman R, Sepanlou SG, Nolte S, Patten S, Weichenthal S, Abera SF, Fereshtehnejad SM, Shiue I, Driscoll T, Vasankari T, Alsharif U, Rahimi-Movaghar V, Vlassov VV, Marcenes WS, Mekonnen W, Melaku YA, Yano Y, Artaman A, Campos I, MacLachlan J, Mueller U, Kim D, Trillini M, Eshrati B, Williams HC, Shibuya K, Dandona R, Murthy K, Cowie B, Amare AT, Antonio CA, Castaneda-Orjuela C, van Gool CH, Violante F, Oh IH, Deribe K, Soreide K, Knibbs L, Kereselidze M, Green M, Cardenas R, Roy N, Tillmann T, Li Y, Krueger H, Monasta L, Dey S, Sheikhbahaei S, Hafezi-Nejad N, Kumar GA, Sreeramareddy CT, Dandona L, Wang H, Vollset SE, Mokdad A, Salomon JA, Lozano R, Vos T, Forouzanfar M, Lopez A, Murray C, Naghavi M. The Global Burden of Cancer 2013. *JAMA oncology* 2015; 1: 505-527.
7. Howlander N, Noone A, Krapcho M, Garshell J, Miller D, Altekruse S. SEER cancer statistics review, 1975–2011. Bethesda, MD: National Cancer Institute; 2014. 2013.
8. Torre LA, Bray F, Siegel RL, Ferlay J, Lortet-Tieulent J, Jemal A. Global cancer statistics, 2012. *CA: a cancer journal for clinicians* 2015; 65: 87-108.
9. Aravalli RN, Steer CJ, Cressman EN. Molecular mechanisms of hepatocellular carcinoma. *Hepatology* 2008; 48: 2047-2063.
10. Craig JR, Peters RL, Edmondson HA, Omata M. Fibrolamellar carcinoma of the liver: a tumor of adolescents and young adults with distinctive

clinico-pathologic features. *Cancer* 1980; 46: 372-379.
11. Wang P, Kang D, Cao W, Wang Y, Liu Z. Diabetes mellitus and risk of hepatocellular carcinoma: a systematic review and meta-analysis. *Diabetes/metabolism research and reviews* 2012; 28: 109-122.
12. Amarapurkar DN, Patel ND, Kamani PM. Impact of diabetes mellitus on outcome of HCC. *Annals of hepatology* 2008; 7: 148-151.
13. Rosenberg L. The risk of liver neoplasia in relation to combined oral contraceptive use. *Contraception* 1991; 43: 643-652.
14. Sherman M. Hepatocellular carcinoma: epidemiology, risk factors, and screening. *Seminars in liver disease* 2005; 25: 143-154.
15. Moradpour D, Blum HE. Pathogenesis of hepatocellular carcinoma. *European journal of gastroenterology & hepatology* 2005; 17: 477-483.
16. Fortini P, Ferretti C, Dogliotti E. The response to DNA damage during differentiation: pathways and consequences. *Mutation research* 2013; 743-744: 160-168.
17. Ogara MF, Sirkin PF, Carcagno AL, Marazita MC, Sonzogni SV, Ceruti JM, Canepa ET. Chromatin relaxation-mediated induction of p19INK4d increases the ability of cells to repair damaged DNA. *PloS one* 2013; 8: e61143.
18. Lee YH, Kuo CY, Stark JM, Shih HM, Ann DK. HP1 promotes tumor suppressor BRCA1 functions during the DNA damage response. *Nucleic acids research* 2013; 41: 5784-5798.
19. Pawlik TM, Poon RT, Abdalla EK, Zorzi D, Ikai I, Curley SA, Nagorney DM, Belghiti J, Ng IO, Yamaoka Y, Lauwers GY, Vauthey JN, International Cooperative Study Group on Hepatocellular C. Critical appraisal of the clinical and pathologic predictors of survival after resection of large hepatocellular carcinoma. *Archives of surgery* 2005; 140: 450-457; discussion 457-458.
20. Seshadri RM, Besur S, Niemeyer DJ, Templin M, McKillop IH, Swan RZ, Martinie JB, Russo MW, Iannitti DA. Survival analysis of patients with stage I and II hepatocellular carcinoma after a liver transplantation or liver resection. *HPB : the official journal of the International Hepato Pancreato Biliary Association* 2014; 16: 1102-1109.
21. Trevisani F, Cantarini MC, Wands JR, Bernardi M. Recent advances in the natural history of hepatocellular carcinoma. *Carcinogenesis* 2008; 29: 1299-1305.
22. Davila JA, Duan Z, McGlynn KA, El-Serag HB. Utilization and outcomes of palliative therapy for hepatocellular carcinoma: a population-based study in the United States. *Journal of clinical gastroenterology* 2012; 46: 71-77.
23. Anthony PP, Vogel CL, Barker LF. Liver cell dysplasia: a premalignant condition. *Journal of clinical pathology* 1973; 26: 217-223.
24. Lee RG, Tsamandas AC, Demetris AJ. Large cell change (liver cell dysplasia) and hepatocellular carcinoma in cirrhosis: matched case-control study, pathological analysis, and pathogenetic hypothesis. *Hepatology* 1997; 26: 1415-1422.
25. Kim H, Oh BK, Roncalli M, Park C, Yoon SM, Yoo JE, Park YN. Large liver cell

change in hepatitis B virus-related liver cirrhosis. *Hepatology* 2009; 50: 752-762.
26. Marchio A, Terris B, Meddeb M, Pineau P, Duverger A, Tiollais P, Bernheim A, Dejean A. Chromosomal abnormalities in liver cell dysplasia detected by comparative genomic hybridisation. *Molecular pathology : MP* 2001; 54: 270-274.
27. Su Q, Bannasch P. Relevance of hepatic preneoplasia for human hepatocarcinogenesis. *Toxicologic pathology* 2003; 31: 126-133.
28. Borzio M, Bruno S, Roncalli M, Mels GC, Ramella G, Borzio F, Leandro G, Servida E, Podda M. Liver cell dysplasia is a major risk factor for hepatocellular carcinoma in cirrhosis: a prospective study. *Gastroenterology* 1995; 108: 812-817.
29. Zhao M, Zhang NX, Du ZY, Laissue JA, Zimmermann A. Three types of liver cell dysplasia (LCD) in small cirrhotic nodules are distinguishable by karyometry and PCNA labelling, and their features resemble distinct grades of hepatocellular carcinoma. *Histology and histopathology* 1994; 9: 73-83.
30. Watanabe S, Okita K, Harada T, Kodama T, Numa Y, Takemoto T, Takahashi T. Morphologic studies of the liver cell dysplasia. *Cancer* 1983; 51: 2197-2205.
31. Ferrell LD, Crawford JM, Dhillon AP, Scheuer PJ, Nakanuma Y. Proposal for standardized criteria for the diagnosis of benign, borderline, and malignant hepatocellular lesions arising in chronic advanced liver disease. *The American journal of surgical pathology* 1993; 17: 1113-1123.
32. Le Bail B, Belleannee G, Bernard PH, Saric J, Balabaud C, Bioulac-Sage P. Adenomatous hyperplasia in cirrhotic livers: histological evaluation, cellular density, and proliferative activity of 35 macronodular lesions in the cirrhotic explants of 10 adult French patients. *Human pathology* 1995; 26: 897-906.
33. Su Q, Benner A, Hofmann WJ, Otto G, Pichlmayr R, Bannasch P. Human hepatic preneoplasia: phenotypes and proliferation kinetics of foci and nodules of altered hepatocytes and their relationship to liver cell dysplasia. *Virchows Archiv : an international journal of pathology* 1997; 431: 391-406.
34. Frese KK, Tuveson DA. Maximizing mouse cancer models. *Nature reviews Cancer* 2007; 7: 645-658.
35. Palmiter RD, Brinster RL, Hammer RE, Trumbauer ME, Rosenfeld MG, Birnberg NC, Evans RM. Dramatic growth of mice that develop from eggs microinjected with metallothionein-growth hormone fusion genes. *Nature* 1982; 300: 611-615.
36. Buendia MA. Genetics of hepatocellular carcinoma. *Seminars in cancer biology* 2000; 10: 185-200.
37. Lee HC, Kim M, Wands JR. Wnt/Frizzled signaling in hepatocellular carcinoma. *Frontiers in bioscience : a journal and virtual library* 2006; 11: 1901-1915.
38. Nantasanti S, Toussaint MJ, Youssef SA, Tooten PC, de Bruin A. Rb and p53 Liver Functions Are Essential for Xenobiotic Metabolism and Tumor Suppression. *PloS one* 2016; 11: e0150064.
39. Ali SH, DeCaprio JA. Cellular transformation by SV40 large T antigen:

interaction with host proteins. *Seminars in cancer biology* 2001; 11: 15-23.
40. Ahuja D, Saenz-Robles MT, Pipas JM. SV40 large T antigen targets multiple cellular pathways to elicit cellular transformation. *Oncogene* 2005; 24: 7729-7745.
41. Horie Y, Suzuki A, Kataoka E, Sasaki T, Hamada K, Sasaki J, Mizuno K, Hasegawa G, Kishimoto H, Iizuka M, Naito M, Enomoto K, Watanabe S, Mak TW, Nakano T. Hepatocyte-specific Pten deficiency results in steatohepatitis and hepatocellular carcinomas. *The Journal of clinical investigation* 2004; 113: 1774-1783.
42. Thorgeirsson SS, Santoni-Rugiu E. Transgenic mouse models in carcinogenesis: interaction of c-myc with transforming growth factor alpha and hepatocyte growth factor in hepatocarcinogenesis. *British journal of clinical pharmacology* 1996; 42: 43-52.
43. Harada N, Oshima H, Katoh M, Tamai Y, Oshima M, Taketo MM. Hepatocarcinogenesis in mice with beta-catenin and Ha-ras gene mutations. *Cancer research* 2004; 64: 48-54.
44. Nicholes K, Guillet S, Tomlinson E, Hillan K, Wright B, Frantz GD, Pham TA, Dillard-Telm L, Tsai SP, Stephan JP, Stinson J, Stewart T, French DM. A mouse model of hepatocellular carcinoma: ectopic expression of fibroblast growth factor 19 in skeletal muscle of transgenic mice. *The American journal of pathology* 2002; 160: 2295-2307.
45. Tonjes RR, Lohler J, O'Sullivan JF, Kay GF, Schmidt GH, Dalemans W, Pavirani A, Paul D. Autocrine mitogen IgEGF cooperates with c-myc or with the Hcs locus during hepatocarcinogenesis in transgenic mice. *Oncogene* 1995; 10: 765-768.
46. Ohgaki H, Sanderson ND, Ton P, Thorgeirsson SS. Molecular analyses of liver tumors in c-myc transgenic mice and c-myc and TGF-alpha double transgenic mice. *Cancer letters* 1996; 106: 43-49.
47. Xiong J, Yao YC, Zi XY, Li JX, Wang XM, Ye XT, Zhao SM, Yan YB, Yu HY, Hu YP. Expression of hepatitis B virus X protein in transgenic mice. *World journal of gastroenterology* 2003; 9: 112-116.
48. Tanaka N, Moriya K, Kiyosawa K, Koike K, Aoyama T. Hepatitis C virus core protein induces spontaneous and persistent activation of peroxisome proliferator-activated receptor alpha in transgenic mice: implications for HCV-associated hepatocarcinogenesis. *International journal of cancer* 2008; 122: 124-131.
49. Clarke R. Human breast cancer cell line xenografts as models of breast cancer. The immunobiologies of recipient mice and the characteristics of several tumorigenic cell lines. *Breast cancer research and treatment* 1996; 39: 69-86.
50. Bankert RB, Egilmez NK, Hess SD. Human-SCID mouse chimeric models for the evaluation of anti-cancer therapies. *Trends in immunology* 2001; 22: 386-393.
51. Wogan GN. Impacts of chemicals on liver cancer risk. *Seminars in cancer biology* 2000; 10: 201-210.
52. Williams GM. Chemicals with carcinogenic activity in the rodent liver;

mechanistic evaluation of human risk. *Cancer letters* 1997; 117: 175-188.
53. Gonzalez FJ. The peroxisome proliferator-activated receptor alpha (PPARalpha): role in hepatocarcinogenesis. *Molecular and cellular endocrinology* 2002; 193: 71-79.
54. Rajewsky MF, Dauber W, Frankenberg H. Liver carcinogenesis by diethylnitrosamine in the rat. *Science* 1966; 152: 83-85.
55. Lee JS, Chu IS, Mikaelyan A, Calvisi DF, Heo J, Reddy JK, Thorgeirsson SS. Application of comparative functional genomics to identify best-fit mouse models to study human cancer. *Nature genetics* 2004; 36: 1306-1311.
56. Verna L, Whysner J, Williams GM. N-nitrosodiethylamine mechanistic data and risk assessment: bioactivation, DNA-adduct formation, mutagenicity, and tumor initiation. *Pharmacology & therapeutics* 1996; 71: 57-81.
57. Williams GM, Iatropoulos MJ, Jeffrey AM. Mechanistic basis for nonlinearities and thresholds in rat liver carcinogenesis by the DNA-reactive carcinogens 2-acetylaminofluorene and diethylnitrosamine. *Toxicologic pathology* 2000; 28: 388-395.
58. Zimmers TA, Jin X, Gutierrez JC, Acosta C, McKillop IH, Pierce RH, Koniaris LG. Effect of in vivo loss of GDF-15 on hepatocellular carcinogenesis. *Journal of cancer research and clinical oncology* 2008; 134: 753-759.
59. Kaestner KH, Knochel W, Martinez DE. Unified nomenclature for the winged helix/forkhead transcription factors. *Genes & development* 2000; 14: 142-146.
60. Jackson BC, Carpenter C, Nebert DW, Vasiliou V. Update of human and mouse forkhead box (FOX) gene families. *Human genomics* 2010; 4: 345-352.
61. Myatt SS, Lam EW. The emerging roles of forkhead box (Fox) proteins in cancer. *Nature reviews Cancer* 2007; 7: 847-859.
62. Biggs WH, 3rd, Cavenee WK, Arden KC. Identification and characterization of members of the FKHR (FOX O) subclass of winged-helix transcription factors in the mouse. *Mammalian genome : official journal of the International Mammalian Genome Society* 2001; 12: 416-425.
63. Hoekman MF, Jacobs FM, Smidt MP, Burbach JP. Spatial and temporal expression of FoxO transcription factors in the developing and adult murine brain. *Gene expression patterns : GEP* 2006; 6: 134-140.
64. Brunet A, Bonni A, Zigmond MJ, Lin MZ, Juo P, Hu LS, Anderson MJ, Arden KC, Blenis J, Greenberg ME. Akt promotes cell survival by phosphorylating and inhibiting a Forkhead transcription factor. *Cell* 1999; 96: 857-868.
65. Jitrapakdee S. Transcription factors and coactivators controlling nutrient and hormonal regulation of hepatic gluconeogenesis. *The international journal of biochemistry & cell biology* 2012; 44: 33-45.
66. Oh KJ, Han HS, Kim MJ, Koo SH. CREB and FoxO1: two transcription factors for the regulation of hepatic gluconeogenesis. *BMB reports* 2013; 46: 567-574.
67. Matsumoto M, Pocai A, Rossetti L, Depinho RA, Accili D. Impaired regulation of hepatic glucose production in mice lacking the forkhead transcription factor Foxo1 in liver. *Cell metabolism* 2007; 6: 208-216.
68. Altomonte J, Richter A, Harbaran S, Suriawinata J, Nakae J, Thung SN, Meseck

M, Accili D, Dong H. Inhibition of Foxo1 function is associated with improved fasting glycemia in diabetic mice. *American journal of physiology Endocrinology and metabolism* 2003; 285: E718-728.

69. Zhang T, Kim DH, Xiao X, Lee S, Gong Z, Muzumdar R, Calabuig-Navarro V, Yamauchi J, Harashima H, Wang R, Bottino R, Alvarez-Perez JC, Garcia-Ocana A, Gittes G, Dong HH. FoxO1 Plays an Important Role in Regulating beta-Cell Compensation for Insulin Resistance in Male Mice. *Endocrinology* 2016; 157: 1055-1070.
70. Okamoto H, Hribal ML, Lin HV, Bennett WR, Ward A, Accili D. Role of the forkhead protein FoxO1 in beta cell compensation to insulin resistance. *The Journal of clinical investigation* 2006; 116: 775-782.
71. Calabuig-Navarro V, Yamauchi J, Lee S, Zhang T, Liu YZ, Sadlek K, Coudriet GM, Piganelli JD, Jiang CL, Miller R, Lowe M, Harashima H, Dong HH. Forkhead Box O6 (FoxO6) Depletion Attenuates Hepatic Gluconeogenesis and Protects against Fat-induced Glucose Disorder in Mice. *The Journal of biological chemistry* 2015; 290: 15581-15594.
72. Xiong X, Tao R, DePinho RA, Dong XC. Deletion of hepatic FoxO1/3/4 genes in mice significantly impacts on glucose metabolism through downregulation of gluconeogenesis and upregulation of glycolysis. *PloS one* 2013; 8: e74340.
73. Gul S. Functional analysis of hepatic FOXO3 signalling in glucose and lipid metabolism. Institute of Physiological Chemistry. Ulm: University of Ulm; 2014.
74. Banerjee A, Meyer K, Mazumdar B, Ray RB, Ray R. Hepatitis C virus differentially modulates activation of forkhead transcription factors and insulin-induced metabolic gene expression. *Journal of virology* 2010; 84: 5936-5946.
75. Deng L, Shoji I, Ogawa W, Kaneda S, Soga T, Jiang DP, Ide YH, Hotta H. Hepatitis C virus infection promotes hepatic gluconeogenesis through an NS5A-mediated, FoxO1-dependent pathway. *Journal of virology* 2011; 85: 8556-8568.
76. Luron L, Saliba D, Blazek K, Lanfrancotti A, Udalova IA. FOXO3 as a new IKK-epsilon-controlled check-point of regulation of IFN-beta expression. *European journal of immunology* 2012; 42: 1030-1037.
77. Honda M, Takehana K, Sakai A, Tagata Y, Shirasaki T, Nishitani S, Muramatsu T, Yamashita T, Nakamoto Y, Mizukoshi E, Sakai Y, Yamashita T, Nakamura M, Shimakami T, Yi M, Lemon SM, Suzuki T, Wakita T, Kaneko S, Hokuriku Liver Study G. Malnutrition impairs interferon signaling through mTOR and FoxO pathways in patients with chronic hepatitis C. *Gastroenterology* 2011; 141: 128-140, 140 e121-122.
78. Tothova Z, Gilliland DG. FoxO transcription factors and stem cell homeostasis: insights from the hematopoietic system. *Cell stem cell* 2007; 1: 140-152.
79. Adachi M, Osawa Y, Uchinami H, Kitamura T, Accili D, Brenner DA. The forkhead transcription factor FoxO1 regulates proliferation and transdifferentiation of hepatic stellate cells. *Gastroenterology* 2007; 132:

1434-1446.
80. You H, Pellegrini M, Tsuchihara K, Yamamoto K, Hacker G, Erlacher M, Villunger A, Mak TW. FOXO3a-dependent regulation of Puma in response to cytokine/growth factor withdrawal. *The Journal of experimental medicine* 2006; 203: 1657-1663.
81. Hu MC, Lee DF, Xia W, Golfman LS, Ou-Yang F, Yang JY, Zou Y, Bao S, Hanada N, Saso H, Kobayashi R, Hung MC. IkappaB kinase promotes tumorigenesis through inhibition of forkhead FOXO3a. *Cell* 2004; 117: 225-237.
82. Guan L, Zhang L, Gong Z, Hou X, Xu Y, Feng X, Wang H, You H. FoxO3 inactivation promotes human cholangiocarcinoma tumorigenesis and chemoresistance via Keap1-Nrf2 signaling. *Hepatology* 2016.
83. Zhang L, Li L, Wei H, Guo L, Ai C, Xu H, Wu Z, Zhou Q. Transcriptional factor FOXO3 negatively regulates the expression of nm23-H1 in non-small cell lung cancer. *Thoracic cancer* 2016; 7: 9-16.
84. Liu H, Yin J, Wang H, Jiang G, Deng M, Zhang G, Bu X, Cai S, Du J, He Z. FOXO3a modulates WNT/beta-catenin signaling and suppresses epithelial-to-mesenchymal transition in prostate cancer cells. *Cellular signalling* 2015; 27: 510-518.
85. Jin Z, Zheng L, Xin X, Li Y, Hua T, Wu T, Wang H. Upregulation of forkhead box O3 transcription is involved in C2-ceramide induced apoptosis and autophagy in ovarian cancer cells in vitro. *Molecular medicine reports* 2014; 10: 3099-3105.
86. Schips TG, Wietelmann A, Hohn K, Schimanski S, Walther P, Braun T, Wirth T, Maier HJ. FoxO3 induces reversible cardiac atrophy and autophagy in a transgenic mouse model. *Cardiovascular research* 2011; 91: 587-597.
87. Schmidt-Strassburger U, Schips TG, Maier HJ, Kloiber K, Mannella F, Braunstein KE, Holzmann K, Ushmorov A, Liebau S, Boeckers TM, Wirth T. Expression of constitutively active FoxO3 in murine forebrain leads to a loss of neural progenitors. *FASEB journal : official publication of the Federation of American Societies for Experimental Biology* 2012; 26: 4990-5001.
88. Descombes P, Chojkier M, Lichtsteiner S, Falvey E, Schibler U. LAP, a novel member of the C/EBP gene family, encodes a liver-enriched transcriptional activator protein. *Genes & development* 1990; 4: 1541-1551.
89. Bullock MD, Bruce A, Sreekumar R, Curtis N, Cheung T, Reading I, Primrose JN, Ottensmeier C, Packham GK, Thomas G, Mirnezami AH. FOXO3 expression during colorectal cancer progression: biomarker potential reflects a tumour suppressor role. *British journal of cancer* 2013; 109: 387-394.
90. Jiang Y, Zou L, Lu WQ, Zhang Y, Shen AG. Foxo3a expression is a prognostic marker in breast cancer. *PloS one* 2013; 8: e70746.
91. Tzivion G, Dobson M, Ramakrishnan G. FoxO transcription factors; Regulation by AKT and 14-3-3 proteins. *Biochimica et biophysica acta* 2011; 1813: 1938-1945.
92. Gross DN, Wan M, Birnbaum MJ. The role of FOXO in the regulation of metabolism. *Current diabetes reports* 2009; 9: 208-214.

93. Park YN. Update on precursor and early lesions of hepatocellular carcinomas. *Archives of pathology & laboratory medicine* 2011; 135: 704-715.
94. Meng X, Franklin DA, Dong J, Zhang Y. MDM2-p53 pathway in hepatocellular carcinoma. *Cancer research* 2014; 74: 7161-7167.
95. Matouk IJ, DeGroot N, Mezan S, Ayesh S, Abu-lail R, Hochberg A, Galun E. The H19 non-coding RNA is essential for human tumor growth. *PloS one* 2007; 2: e845.
96. Schlaeger C, Longerich T, Schiller C, Bewerunge P, Mehrabi A, Toedt G, Kleeff J, Ehemann V, Eils R, Lichter P, Schirmacher P, Radlwimmer B. Etiology-dependent molecular mechanisms in human hepatocarcinogenesis. *Hepatology* 2008; 47: 511-520.
97. Ye H, Zhang C, Wang BJ, Tan XH, Zhang WP, Teng Y, Yang X. Synergistic function of Kras mutation and HBx in initiation and progression of hepatocellular carcinoma in mice. *Oncogene* 2014; 33: 5133-5138.
98. Libbrecht L, Severi T, Cassiman D, Vander Borght S, Pirenne J, Nevens F, Verslype C, van Pelt J, Roskams T. Glypican-3 expression distinguishes small hepatocellular carcinomas from cirrhosis, dysplastic nodules, and focal nodular hyperplasia-like nodules. *The American journal of surgical pathology* 2006; 30: 1405-1411.
99. Petersen BE, Zajac VF, Michalopoulos GK. Hepatic oval cell activation in response to injury following chemically induced periportal or pericentral damage in rats. *Hepatology* 1998; 27: 1030-1038.
100. Oh SH, Hatch HM, Petersen BE. Hepatic oval 'stem' cell in liver regeneration. *Seminars in cell & developmental biology* 2002; 13: 405-409.
101. Scholzen T, Gerdes J. The Ki-67 protein: from the known and the unknown. *Journal of cellular physiology* 2000; 182: 311-322.
102. Hans F, Dimitrov S. Histone H3 phosphorylation and cell division. *Oncogene* 2001; 20: 3021-3027.
103. Shaw PH. The role of p53 in cell cycle regulation. *Pathology, research and practice* 1996; 192: 669-675.
104. Parry P, Wei Y, Evans G. Cloning and characterization of the t(X;11) breakpoint from a leukemic cell line identify a new member of the forkhead gene family. *Genes, chromosomes & cancer* 1994; 11: 79-84.
105. Davis RJ, D'Cruz CM, Lovell MA, Biegel JA, Barr FG. Fusion of PAX7 to FKHR by the variant t(1;13)(p36;q14) translocation in alveolar rhabdomyosarcoma. *Cancer research* 1994; 54: 2869-2872.
106. Notas G, Alexaki VI, Kampa M, Pelekanou V, Charalampopoulos I, Sabour-Alaoui S, Pediaditakis I, Dessirier V, Gravanis A, Stathopoulos EN, Tsapis A, Castanas E. APRIL binding to BCMA activates a JNK2-FOXO3-GADD45 pathway and induces a G2/M cell growth arrest in liver cells. *Journal of immunology* 2012; 189: 4748-4758.
107. Carbajo-Pescador S, Steinmetz C, Kashyap A, Lorenz S, Mauriz JL, Heise M, Galle PR, Gonzalez-Gallego J, Strand S. Melatonin induces transcriptional regulation of Bim by FoxO3a in HepG2 cells. *British journal of cancer* 2013;

108: 442-449.
108. Jensen KS, Binderup T, Jensen KT, Therkelsen I, Borup R, Nilsson E, Multhaupt H, Bouchard C, Quistorff B, Kjaer A, Landberg G, Staller P. FoxO3A promotes metabolic adaptation to hypoxia by antagonizing Myc function. *The EMBO journal* 2011; 30: 4554-4570.
109. Castrillon DH, Miao L, Kollipara R, Horner JW, DePinho RA. Suppression of ovarian follicle activation in mice by the transcription factor Foxo3a. *Science* 2003; 301: 215-218.
110. Nakae J, Kitamura T, Kitamura Y, Biggs WH, 3rd, Arden KC, Accili D. The forkhead transcription factor Foxo1 regulates adipocyte differentiation. *Developmental cell* 2003; 4: 119-129.
111. Kitamura T, Nakae J, Kitamura Y, Kido Y, Biggs WH, 3rd, Wright CV, White MF, Arden KC, Accili D. The forkhead transcription factor Foxo1 links insulin signaling to Pdx1 regulation of pancreatic beta cell growth. *The Journal of clinical investigation* 2002; 110: 1839-1847.
112. Hribal ML, Nakae J, Kitamura T, Shutter JR, Accili D. Regulation of insulin-like growth factor-dependent myoblast differentiation by Foxo forkhead transcription factors. *The Journal of cell biology* 2003; 162: 535-541.
113. Plentz RR, Park YN, Lechel A, Kim H, Nellessen F, Langkopf BH, Wilkens L, Destro A, Fiamengo B, Manns MP, Roncalli M, Rudolph KL. Telomere shortening and inactivation of cell cycle checkpoints characterize human hepatocarcinogenesis. *Hepatology* 2007; 45: 968-976.
114. Tiniakos DG, Brunt EM. Proliferating cell nuclear antigen and Ki-67 labeling in hepatocellular nodules: a comparative study. *Liver* 1999; 19: 58-68.
115. Schramek D, Kotsinas A, Meixner A, Wada T, Elling U, Pospisilik JA, Neely GG, Zwick RH, Sigl V, Forni G, Serrano M, Gorgoulis VG, Penninger JM. The stress kinase MKK7 couples oncogenic stress to p53 stability and tumor suppression. *Nature genetics* 2011; 43: 212-219.
116. Chen CL, Tsukamoto H, Machida K. Oncogenic signaling pathways and origins of tumor-initiating stem-like cells of hepatocellular carcinomas induced by hepatitis C virus, alcohol and/or obesity. *Hepatology international* 2014; 8: 330-338.
117. Yang W, Yan HX, Chen L, Liu Q, He YQ, Yu LX, Zhang SH, Huang DD, Tang L, Kong XN, Chen C, Liu SQ, Wu MC, Wang HY. Wnt/beta-catenin signaling contributes to activation of normal and tumorigenic liver progenitor cells. *Cancer research* 2008; 68: 4287-4295.
118. Li D, Cen J, Chen X, Conway EM, Ji Y, Hui L. Hepatic loss of survivin impairs postnatal liver development and promotes expansion of hepatic progenitor cells in mice. *Hepatology* 2013; 58: 2109-2121.
119. Branzei D, Foiani M. Regulation of DNA repair throughout the cell cycle. *Nature reviews Molecular cell biology* 2008; 9: 297-308.
120. Hagenbuchner J, Kuznetsov A, Hermann M, Hausott B, Obexer P, Ausserlechner MJ. FOXO3-induced reactive oxygen species are regulated by BCL2L11 (Bim) and SESN3. *Journal of cell science* 2012; 125: 1191-1203.

121. Hagenbuchner J, Ausserlechner MJ. Mitochondria and FOXO3: breath or die. *Frontiers in physiology* 2013; 4: 147.

8. CURRICULUM VITAE

Persönliche Daten

Name:	Miao Lu
Geburtstag:	20.04.1988 in Jiangsu, VR China
Anschrift:	Tel.: +49 15166124641 e-mail: lumiao_tum@sina.com lumiao_lu@tum.com
Familienstand:	ledig

Schulbildung

09.1994 – 06.1999	Grundschule in Jiangsu
09.1998 – 06.2005	Besuch der Mittelschule in Jiangsu
09.2005 – 06.2012	Studium an der Südost-Universität Nanjing

Ausbildung

09.2005 – 06.2010	Studium an der Südost-Universität Nanjing Studienfach: Klinische Medizin Abschluss: Bachelor-Titel für Medizin
09.2010 – 06.2012	Studium an der Südost-Universität Nanjing Studenfach: allgemeine Chirurgie Abschluss: Master-Titel für Medizin
12.2012 – 07.2016	Studium am Klinikum rechts der Isar München Studienfach: allgemeine Chirurgie

Praktika

07.2008	klinisches Praktikum am Bengbusanyuan Krankenhaus in Bengbu
07.2009 – 06.2010	klinisches Praktikum am Drumtower Krankenhaus in Nanjing
09.2010-03.2012	klinisches Praktikum für allgemeine Chirurgie am Zhongda Krankenhaus in Nanjing

Sonstige Qualifikationen

Sprachkenntnisse:	Chinesisch (Muttersprache) Englisch fließend Deutsch Grundkenntnisse
EDV-Kenntnisse:	Word Excel PowerPoint und SPSS

9. LIST OF PUBLICATIONS

1. Zheng K, Bortuzzo JA, Liu Y, Li W, Pischetsrieder M, Roether J, **Lu M**, Boccaccini AR. Bio-templated bioactive glass particles with hierarchical macro-nano porous structure and drug delivery capability. *Colloids and surfaces B, Biointerfaces* 2015; 135: 825-832

2. Zheng K, **Lu M**, Liu Y, Chen Q, Taccardi N, Huser N, Boccaccini AR. Monodispersed lysozyme-functionalized bioactive glass nanoparticles with antibacterial and anticancer activities. *Biomedical materials* 2016; 11: 035012.

3. Sunami Y, Ringelhan M, Kokai E, **Lu M**, O'Connor T, Lorentzen A, Weber A, Rodewald AK, Mullhaupt B, Terracciano L, Gul S, Wissel S, Leithauser F, Krappmann D, Riedl P, Hartmann D, Schirmbeck R, Strnad P, Huser N, Kleeff J, Friess H, Schmid RM, Geisler F, Wirth T, Heikenwalder M. Canonical NF-kappaB signaling in hepatocytes acts as a tumor-suppressor in hepatitis B virus surface antigen-driven hepatocellular carcinoma by controlling the unfolded protein response. *Hepatology* 2016; 63: 1592-1607.

10. ACKNOWLEDGEMENT

My sincere thanks go to my supervisors Prof. Dr. med. Helmut Friess and PD Dr. med. Norbert Hüser. They provided me with a comfortable environment in which to conduct research.

Special thanks go to my mentor Dr. Yoshiaki Sunami, who provided me with this project and devote a lot to this project. He showed me how to do the experiments and spend a lot of time supervising my project.

I would like to thank Dr. Dr. Daniel Hartmann, who is always enthusiastic and always provides many helpful comments on my research.

I want to thank Prof. Dr. Joerg Kleeff, Susanne Raulefs and Dr. Ivonne Regel. They organized the lab and are always happy to help me when I have questions.

I would also like to thank my colleagues Dr. Lei Liu, Mr. Tao Cheng, Ms. Ziying Jian, Mr. Chengjia Qian, and Dr. Weiwei Wu. I have had a lot of fun working with them.

I would also like to thank our technicians, Nadja Maeritz and Manja Thorwirth. They are key persons who keep the lab running, and they can always help me out of any trouble in my experiments.

Finally, I sincerely thank my family for supporting me when I am out of money, encouraging me when I distrust myself comforting me when I am frustrated. I could not finish my studies without their constant support.